PHYSICAL REVIEW D **90,** 115028 (2014)

Debye screening mass near deconfinement from holography

S. I. Finazzo[*] and J. Noronha[†]

Instituto de Física, Universidade de São Paulo, São Paulo, São Paulo, Brazil

(Received 8 December 2014; published 30 December 2014)

In this paper the smallest thermal screening mass associated with the correlator of the CT-odd operator, $\sim \mathrm{Tr}F_{\mu\nu}\tilde{F}^{\mu\nu}$, is determined in strongly coupled non-Abelian gauge plasmas which are holographically dual to nonconformal, bottom-up Einstein + scalar gravity theories. These holographic models are constructed to describe the thermodynamical properties of $\mathrm{SU}(N_c)$ plasmas near deconfinement at large N_c, and we identify this thermal mass with the Debye screening mass m_D. In this class of nonconformal models with a first-order deconfinement transition at T_c the Debye screening mass m_D displays the same behavior found for the expectation value of the Polyakov loop (which we also compute) jumping from zero below T_c to a nonzero value just above the transition. In the case of a crossover phase transition, m_D/T has a minimum similar to that found for the speed of sound squared c_s^2. This holographic framework is also used to evaluate m_D as a function of η/s in a strongly coupled conformal gauge plasma dual to Gauss–Bonnet gravity. In this case, m_D/T decreases with increasing η/s in accordance with extrapolations from weak coupling calculations.

DOI: 10.1103/PhysRevD.90.115028 PACS numbers: 11.25.Tq, 12.38.Mh

I. INTRODUCTION

In the deconfined phase of non-Abelian gauge theories, the inverse of the Debye screening mass, m_D^{-1}, can be used to define a screening length of the thermal medium that roughly signals the effective maximum interaction distance between two colored heavy probes. Debye screening is the mechanism behind Matsui and Satz's well-known proposal [1] that the "melting" (dissociation) of heavy quarkonia states in the quark-gluon plasma (QGP) is a signature of deconfinement.

Although in weakly coupled Abelian and non-Abelian plasmas the Debye screening mass has been calculated long ago at one loop in perturbation theory [2–4], higher-order perturbative calculations [5–8] indicate the breakdown of the perturbation series expansion for this quantity. Thus, a nonperturbative, gauge invariant definition of the Debye screening mass is needed. A definition that is inherently nonperturbative and gauge invariant was proposed by Arnold and Yaffe in Ref. [9] where m_D was defined as the largest inverse screening length among all the possible Euclidean correlation functions involving pairs of CT-odd operators in the thermal gauge field theory. Previous studies concerning thermal screening lengths in non-Abelian plasmas include lattice calculations [10–16], nonperturbative analyses of the gluon propagator at finite temperature [17–20], other analytical approaches [21,22], and holographic calculations [23–25].

In this paper we use the gauge/gravity duality [26–29] to understand the general properties of the smallest thermal screening mass associated with the CT-odd operator, $\sim \mathrm{Tr}F_{\mu\nu}\tilde{F}^{\mu\nu}$, in nonconformal strongly coupled plasmas described by Einstein gravity plus a scalar field. We shall follow Ref. [23] and *identify* this thermal screening mass as the Debye mass m_D in the strongly coupled plasma. After associating this Debye screening mass in the field theory with the lowest lying mass in the spectrum [30,31] of axion fluctuations in the bulk [23], we show (given some reasonable conditions regarding the axion effective action) that the bulk axion spectrum is gapped, positive, and discrete in the deconfined phase of these theories. This shows that this thermal screening radius, which may be relevant for the melting of heavy quarkonia in this class of strongly coupled large-N_c plasmas, is necessarily finite (even in the case of a second-order deconfining transition). Also, we find that m_D/T generally follows the behavior of the expectation value of the Polyakov-loop operator near the phase transition. In fact, for a first-order deconfinement phase transition, m_D/T jumps from zero below the critical temperature T_c to a finite value immediately above it.

To estimate the behavior of this screening mass in a nonconformal strongly coupled plasma with similar properties to the QCD plasma, we consider a variety of holographic bottom-up models constructed using five-dimensional Einstein + scalar effective bulk actions. The first model, which we call model A, is built in the context of improved holographic QCD (IHQCD) [32–36], being a simple analytical model [37] involving an Einstein + scalar gravity bulk action dual to a strongly coupled non-Abelian which possesses a first-order confinement/deconfinement phase transition. The second class of models (model B) [38–40] is also based on Einstein + scalar bulk actions, but now the scalar potentials are chosen in order to reproduce some lattice QCD thermodynamical results. The model that reproduces lattice data for pure $\mathrm{SU}(3)$ Yang–Mills, which possesses a first-order deconfinement transition [41–43], is

[*]stefano@if.usp.br
[†]noronha@if.usp.br

called model B1, whereas the model that matches lattice data for QCD with $(2+1)$ light flavors of quarks [44] is called model B2. For all models, A, B1, and B2, we obtain, numerically, the screening mass m_D as a function of the temperature T. For models A and B1, both of which present a first-order phase transition, we explicitly verify the existence of a discontinuity in m_D/T at the critical temperature T_c, where m_D/T jumps discontinuously from 0 to a finite value above T_c. For model B2, which displays a crossover phase transition, m_D/T increases with T smoothly from zero and has a local minimum at a given temperature (following a behavior similar to that shown by the speed of sound), after which it then continuously rises to its conformal limit.

As a final application, we consider the screening mass in a strongly coupled conformal plasma dual to Gauss–Bonnet gravity [45,46]. In this theory the shear viscosity to entropy density ratio, η/s, is different than $1/(4\pi)$ [47–49] for a range of values of the controlling parameter of the theory, $\lambda_{\rm GB}$, associated with the higher-order derivatives in the action as shown in Refs. [50,51]. Thus, in this case one can see how m_D/T depends upon η/s in this strongly coupled plasma and compare with the results of the phenomenological approach based on fits to the heavy quark potential at strong coupling pursued in Ref. [52]. We find the intriguing result that m_D/T decreases with increasing η/s.

This paper is organized as follows. In Sec. II we motivate the nonperturbative definition of thermal screening lengths in non-Abelian gauge theories (the reader that is already familiar with Ref. [9] may want to skip the introductory Secs. II A and II B and go directly to Sec. II C) and present the holographic prescription for evaluating these quantities in strongly coupled plasmas dual to bottom-up theories of gravity involving the metric and a scalar field. In this section we also present some general results for the thermal screening mass associated with $\mathrm{Tr}F_{\mu\nu}\tilde{F}^{\mu\nu}$ which are valid in this holographic framework. In Sec. III we briefly review the results and techniques of Refs. [23,30,31] for evaluating this thermal screening mass in a strongly coupled $\mathcal{N}=4$ super Yang-Mills (SYM) plasma. Section IV is dedicated to the evaluation of m_D and the Polyakov loop in model A. In Sec. V we review some general results for the B class of models pertinent to our purposes. Section VI (Sec. VII) is reserved for the evaluation of m_D in the B1 model (B2 model, respectively). We show that the heavy quark free energy (extracted from the expectation value of the Polyakov loop) in these holographic models for $\mathrm{SU}(N_c)$ Yang–Mills theory nicely describes recent lattice data [53]. In Sec. VIII we analyze $m_D \times \eta/s$ in Gauss–Bonnet gravity. Section IX contains our conclusions and outlook.[1]

[1]In Appendix A we present the technical details of a coordinate change used in the study of the B models. We also present the evaluation of the glueball spectrum at $T=0$ in model B1 in Appendix B.

II. GENERAL RESULTS FOR THE HOLOGRAPHIC DEBYE SCREENING MASS

For the sake of completeness, in Secs. II A and II B, we review some necessary results on screening lengths in thermal gauge theories and the nonperturbative definition of the Debye screening mass proposed in Ref. [9]. Then, in Sec. II C we motivate the holographic prescription for the evaluation of the Debye mass and study some of its general properties using holography.

A. Screening lengths in thermal gauge theories

Let $\hat{O}$ be a gauge invariant operator and consider the (equal-time) Euclidean two-point correlation function

$$G_E(\vec{x}) \equiv \langle 0|\hat{O}^\dagger(\vec{x})\hat{O}(\vec{0})|0\rangle. \tag{1}$$

A quantum field theory (QFT) in thermal equilibrium can, as usual, be studied using the Matsubara (or imaginary time) formalism [4], where we consider the compactification of the imaginary time $\tau = it$ direction in a circle of radius $\beta = 1/T$, where T is the temperature of the thermal bath. A key insight to this discussion [9,23] is that the resulting Euclidean symmetry allows us, instead of compactifying along the time direction, to compactify along any of the spatial directions; for instance, we may compactify along the x spatial direction. Let $\{|n\rangle\}$ be a complete set of eigenstates of the translation operator H_E along the x direction, with corresponding eigenvalues E_n. Then, inserting the completeness relation for the basis $\{|n\rangle\}$, one finds

$$G_E(x) = \sum_{n=0}^{\infty}\langle 0|\hat{O}^\dagger(x)|n\rangle\langle n|\hat{O}(0)|0\rangle. \tag{2}$$

Since H_E is a Euclidean translation operator,

$$\hat{O}(x) = e^{H_E|x|}\hat{O}(0)e^{-H_E|x|}, \tag{3}$$

and, thus,

$$G_E(x) = \sum_{n=0}^{\infty} e^{-E_n|x|}|c_n|^2, \tag{4}$$

where

$$c_n \equiv \langle n|\hat{O}(0)|0\rangle. \tag{5}$$

For large spatial separations, the ground state contribution to Eq. (4) dominates, and

$$G_E(x) \sim e^{-E_0|x|}|c_0|^2. \tag{6}$$

Thus, E_0^{-1} may be taken as the screening length of $G_E(x)$—for distances $|x|$ greater than E_0^{-1}, the fluctuations of $\hat{O}$ are effectively not correlated.

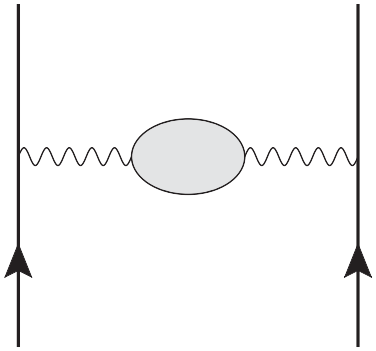

FIG. 1. Perturbative definition of the Debye mass. A single photon (gluon) is exchanged between two static test charges. The pole of the photon (gluon) propagator at zero frequency gives the Debye screening mass m_D, the inverse screening length of the static potential.

B. Nonperturbative definition of the Debye screening mass

In this section we briefly review the nonperturbative definition of the Debye screening mass proposed in Ref. [9].

In QED, perturbatively, the Debye screening mass m_D can be determined as the pole in the 00 component of the photon propagator at zero frequency, $\Pi_{00}(0,\vec{p}^2)$ (Fig. 1)—i.e., the solution of

$$\Pi_{00}(0,\vec{p}^2=-m_D^2)+m_D^2=0. \tag{7}$$

The screening length of the static potential of two static test charges is given by the inverse Debye mass m_D^{-1}. Magnetic fields are unscreened in perturbation theory so that $\Pi_{ij}\to 0$ as $\vec{p}\to 0$—the Debye screening mass captures the physics of electric screening. This definition can be applied perturbatively to non-Abelian gauge theories, yielding the lowest-order, one-loop, perturbative result in the ultrarelativistic approximation (neglecting particle masses and chemical potentials) [2–4]

$$m_D=\sqrt{\frac{N_c}{3}+\frac{N_f}{3}}gT+O(g^2T), \tag{8}$$

for an SU(N_c) gauge theory with N_f minimally coupled fermions, where g is the gauge theory coupling constant.

Reference [9] proposed a way to define the Debye screening mass in an explicit gauge invariant (and nonperturbative) manner using Euclidean time reflection symmetry that is useful in the context of strongly coupled plasmas. Consider the CT (the composite of time reversal T and charge conjugation C) transformation in real time. The corresponding symmetry in Euclidean time is R_τ, where R_τ is the imaginary (Euclidean) time reflection. To see this, note that any Lorentz invariant theory must have CPT symmetry, where P stands for spatial inversion. Correspondingly, any Euclidean invariant theory must be rotation invariant. Since PR_τ is a pure rotation in an Euclidean theory, CPT must correspond to PR_τ. Also, given that P is time independent, R_τ must correspond to CT. Since A_0 is even under R_τ and $\vec{A}$ is odd under R_τ, the authors of Ref. [9] defined the Debye screening mass m_D as the inverse of the largest correlation length (or, equivalently, the smallest screening mass) of all correlation functions $\langle\hat{A}(\vec{x})\hat{B}(\vec{0})\rangle$ involving two local, gauge invariant operators $\hat{A}$, $\hat{B}$, both odd under Euclidean time reflection R_τ (CT in real time). This construction explicitly removes the magnetic gluon exchange and takes into account only the chromoelectric gluons. Thus, according to Ref. [9], the Debye screening mass may be defined as the largest inverse screening length in this channel:

$$G_E(\vec{x})=\langle\hat{A}(\vec{x})\hat{B}(\vec{0})\rangle\sim e^{-m_D|\vec{x}|}\quad\text{as } |\vec{x}|\to\infty. \tag{9}$$

In this paper we will adopt this definition of the Debye screening mass since it can be readily used in the case of strongly coupled plasmas that are holographically dual to theories of gravity, as shown in Ref. [23]. From the preceding discussion, we see that to evaluate this Debye screening mass one has to determine correlation lengths of two-point functions in a non-Abelian plasma—or, equivalently, evaluate the smallest R_τ odd glueball mass in a three-dimensional Yang–Mills theory at zero temperature. From the holographic standpoint, the extraction of the glueball masses in the large N_c and strong coupling limit was done in Refs. [30,31]. The holographic prescription for evaluating the glueball masses corresponds to analyzing in the theory of gravity dual to the QFT in question the fluctuations of the bulk fields that source, in the corresponding gauge theory, the gauge invariant operators that couple to the glueballs which have the same quantum numbers of the dual bulk field.

In the case of the $J^{\mathrm{PC}}=0^{-+}$ channel (which is R_τ odd), according to the IHQCD framework [32,33,54], one must analyze the dimension-4 operator $\mathrm{Tr}F_{\mu\nu}\tilde{F}^{\mu\nu}$ which is sourced by a massless (pseudoscalar) axion field $a(x,z)$ in the bulk. Then, as discussed in Ref. [23], the Debye mass corresponds to the imaginary wave vector of smallest magnitude for which the equations of motion corresponding to the axion fluctuations admit plane wave solutions of the kind $e^{i\vec{k}\cdot\vec{x}}a(z)$ that are regular at the horizon and obey a Dirichlet condition at the boundary [55].

A direct consequence of this definition of the Debye screening mass in holographic strongly coupled plasmas is that this m_D is independent of the gauge coupling and the number of colors when both of them are sufficiently large. In fact, since this m_D is determined by the bulk fluctuations of the axion in a supergravitylike action, this quantity cannot depend on the gauge coupling (since for a two derivative action there are no terms including the string

scale ℓ_s) nor the number of colors (which only appears in this case as an overall multiplicative factor in the action in the form of the five-dimensional Newton's constant). This should be kept in mind when one tries to make a connection between these strongly coupled results and the general intuition acquired over the years about the Debye mass computed within perturbation theory. For instance, we shall show below that this m_D is never zero in the deconfined phase of the strongly coupled plasma, which is described by a black brane in the bulk. Therefore, even in the case of a second-order phase transition, the m_D we compute would be nonzero. Thus, one cannot directly identify this quantity with the one that describes the fluctuations of Polyakov loops in effective models for the QGP [56–59].

C. General properties of the holographic axion spectrum

Armed with the holographic prescription for extracting the Debye screening mass by means of the bulk axion spectrum, we now examine some of its general properties in a large class of gravity duals. The action for the fluctuations of the massless axion in these backgrounds is assumed to be of the form[2]

$$S = \frac{1}{32\pi G_5}\int d^5x\sqrt{g}(\mathcal{Z}(z)g^{\mu\nu}\partial_\mu a\partial_\nu a), \tag{10}$$

where $G_5 \sim 1/N_c^2$ is the five-dimensional gravitational constant and $\mathcal{Z}(z)$ is a given function of the holographic coordinate z—the reason for including this axion coupling function is that in certain classes of backgrounds, as in those of improved holographic QCD [32–36], a resummation of the contributions originating from string theory should result in an effective action for the axion that involves this multiplicative factor. The specific form for this function will be defined later in the paper.

The background metric for the asymptotically five dimensional Anti-de Sitter (AdS_5) space-time (with conformal boundary at $z \to 0$) is defined by the line element

$$ds^2 = e^{2\mathcal{A}(z)}\left(f(z)d\tau^2 + d\vec{x}^2 + \frac{dz^2}{f(z)}\right), \tag{11}$$

where $f(0) = 1$ and the black brane horizon z_h is the smallest root of $f(z_h) = 0$. Moreover, note that $\lim_{z\to 0} e^{2\mathcal{A}(z)} = R^2/z^2$ where R is the radius of the asymptotic AdS_5 space. The equation of motion for the axion is

$$\partial_\mu(\mathcal{Z}(z)e^{5\mathcal{A}}g^{\mu\nu}\partial_\nu a) = 0, \tag{12}$$

[2]Note that, since in IHQCD the bulk axion is trivial in the background, the action for its fluctuations is easily determined to be the one in (10) [54].

and, in momentum space (taking the Matsubara frequency to zero since we want the largest inverse correlation length) with the plane wave ansatz $a(\vec{x}, z) \to e^{i\vec{k}\cdot\vec{x}}a(z)$, one finds the equation of motion (with $M^2 = -\vec{k}^2$),

$$\partial_z(e^{2\mathcal{B}}f(z)a') + M^2e^{2\mathcal{B}}a = 0, \tag{13}$$

where $a'(z) = da(z)/dz$ and we have defined the function

$$\mathcal{B}(z) \equiv \frac{3}{2}\mathcal{A}(z) + \frac{1}{2}\log\mathcal{Z}(z). \tag{14}$$

An alternative, but useful, form of the equation of motion is obtained by introducing $\psi = e^{\mathcal{B}}a$, which leads to

$$-\psi'' - \frac{f'}{f}\psi' + \frac{1}{f}[f(\mathcal{B}'^2 + \mathcal{B}'') + f'\mathcal{B}']\psi = \frac{M^2}{f}\psi. \tag{15}$$

This form of the equation of motion is especially useful at zero temperature where $f = 1$. In this case, we have the Schrödinger-like equation

$$-\psi'' + \mathcal{V}(z)\psi = M^2\psi, \tag{16}$$

where the potential $\mathcal{V}$ is defined as

$$\mathcal{V}(z) = \mathcal{B}'(z)^2 + \mathcal{B}''(z). \tag{17}$$

The pole of the corresponding Euclidean Green's function is obtained by imposing a Dirichlet condition for the fluctuation at the boundary while at the horizon z_h the axion fluctuation must be finite. This completely specifies the eigenvalue problem to find M^2.

Let us now state some basic facts about the bulk axion spectrum in these theories. First, M^2 is real. Second, the spectrum is gapped ($M^2 > 0$) if there is a black brane horizon in the bulk. Third, the spectrum is discrete.

That the spectrum is purely real follows simply from the fact that Eq. (13) and its boundary conditions are posed as a Sturm–Liouville problem.

Now, let us analyze the mass gap. It is easy to see $M = 0$ is not in the spectrum. If $M = 0$, then the equation of motion (13) can be easily integrated yielding two linearly independent solutions, $a \propto \text{const}$ and $a \propto \int dz e^{-2\mathcal{B}}f^{-1}$. The solution $a \propto \text{constant} \neq 0$ is not normalizable in the UV and must be discarded. The other solution is normalizable; however, near the horizon, as $f(z) \sim -|f'(z_h)|(z_h - z)$ and $\mathcal{B} \sim \mathcal{B}(z_h)$, $a \propto \log(z - z_h) \to \infty$. Thus, the normalizable solution in the UV is not finite on the horizon. Thus, $M = 0$ does not satisfy the boundary conditions and is not in spectrum if there is a horizon.

To prove that $M^2 < 0$ is not allowed, we employ an argument used by Witten [28]. The equation of motion (13) can be obtained from the on-shell action

$$\frac{1}{32\pi G_5 T}\int_0^{z_h} dz\mathcal{Z}(z)e^{3\mathcal{A}}[f(\partial_z a)^2 - M^2 a^2]. \tag{18}$$

If a is a normalizable solution of the equations of motion, then after integrating Eq. (18) by parts one sees that it must vanish. Now, suppose that $M^2 < 0$. Then in Eq. (18) both terms are strictly positive. Thus, we must have $da/dz = 0$ and $a = 0$, since the solution is normalizable. This is just the trivial solution, and, thus, $M^2 < 0$ cannot be an eigenvalue of the equation of motion. Therefore, as we have already shown that $M \neq 0$, we see that $M^2 > 0$. This shows the existence of the mass gap.

Finally, intuitively, the spectrum must be discrete—the axion is confined into an asymptotically AdS_5 space-time with a black brane deep in the bulk. The Dirichlet asymptotic boundary and the horizon work as two "walls" that confine the axion into an infinite well, hence the discrete spectrum.

III. DEBYE SCREENING MASS IN STRONGLY COUPLED $\mathcal{N} = 4$ SYM THEORY

A. Axion spectrum

In this section we review the holographic evaluation of the Debye mass (i.e., the smallest thermal mass associated with axion fluctuations in the bulk) in a strongly coupled $\mathcal{N} = 4$ SYM plasma by means of the gauge/gravity duality [23]. Since the dilaton is constant in this case, the equations of motion for the dilaton and the axion fluctuations are degenerate. Also, the $\mathcal{Z}$ function is constant, and one can set it to unity since one can consistently set the other bulk fields in type IIB supergravity, apart from the metric and the five-form F_5, to be trivial. Thus, one can simply retrieve the result from Ref. [30] for the spectrum of a massless scalar field in a Schwarzschild AdS_5 background. The final result for the ground state is given by Ref. [23],

$$m_D = c\pi T, \tag{19}$$

where $c = 3.4041$. Since the analytical and numerical procedures used in this case will be applied with minimal changes in the next two sections, it will be useful to review here the numerical procedure used to determine the constant c defined above in some detail.

For the AdS_5 Schwarzchild background, the black brane temperature is $T = \pi R^2 z_h$. The equation of motion is given by Eq. (15); it is useful to write it in terms of the normalized variable $u = z/z_h = \pi R^2 T z$ and the dimensionless mass $\tilde{M} = M/(\pi T)$. We need to match the solution of the equation of motion Eq. (15) with the asymptotic equation of motion near the boundary $u \to 0$,

$$-\frac{d^2\psi}{du^2} + \mathcal{V}_{\text{asy}}\psi = \tilde{M}^2\psi, \tag{20}$$

with the asymptotic potential $\mathcal{V}_{\text{asy}}(u) = \mathcal{V}(u \to 0) = 15/(4u^2)$ [see Eq. (17)]. The general solution of the asymptotic equation (20) is

$$\psi(u) = C_1\sqrt{u}[J_2(\tilde{M}u) + C_2 Y_2(\tilde{M}u)], \tag{21}$$

where J_n and Y_n are Bessel functions of the first and second kind, respectively, and C_1, C_2 are integration constants. Since Y_2 does not vanish at the boundary, we pick J_2 as the asymptotic solution setting $C_2 = 0$. The coefficient C_1 is chosen to fix the leading coefficient of the series expansion of the Bessel function to 1; then $C_1 = M^2/8$. Thus, at the boundary, the full solution ψ must match the asymptotic solution

$$\begin{aligned}\psi_{\text{asy}}(u) &= \frac{8\sqrt{u}}{\tilde{M}^2}J_2(\tilde{M}u) \\ &= u^{5/2} - \frac{1}{12}\tilde{M}^2 u^{9/2} + \frac{1}{384}\tilde{M}^4 u^{13/2} + \mathcal{O}(\tilde{M}^6 u^{17/2}).\end{aligned} \tag{22}$$

To obtain the axion spectrum numerically, we use a shooting procedure. One starts with an initial value for $\tilde{M}^2$ and numerically solves the equation of motion (15) imposing as boundary conditions that the solution $\psi(u)$ matches the asymptotic solution (22) and its first derivative for some $u_0 \ll 1$. One then integrates the initial value problem up to near the horizon. When $\tilde{M}^2$ is not an exact eigenvalue, $\psi(u)$ diverges at the horizon. However, $\psi(u \to 1)$ changes sign when one passes by an exact eigenvalue, and, thus, one can bracket it by scanning when such sign change happens. Care must be taken to certify that one has not missed the ground state (or an excited state) by starting with values of $\tilde{M}^2$ only slightly above zero. Proceeding this way, one obtains for the ground state of the axion spectrum $\tilde{M} = m_D/(\pi T)$ the result (19).

IV. DEBYE SCREENING MASS IN MODEL A

A. General IHQCD backgrounds

The IHQCD model for $SU(N_c)$ Yang–Mills theory proposed in Refs. [32–36] corresponds to writing the most general gravitational effective action involving the metric (which is dual to the energy-momentum tensor of the gauge theory) and the dilaton ϕ (dual to the dimension-4 scalar glueball operator $\text{Tr}F^2$ in the gauge theory) with at most two derivatives in the bulk. In this model, e^{ϕ} is related to the gauge coupling. The effective five-dimensional action in the Einstein frame for the metric and the dilaton in IHQCD is

$$S = \frac{1}{16\pi G_5}\int d^5x\sqrt{g}\left[\mathcal{R} - \frac{4}{3}(\partial\phi)^2 + V(\phi)\right], \tag{23}$$

plus a Gibbons–Hawking boundary term, necessary to give a well-posed variational problem (this term and other contributions needed in the process of holographic renormalization [60,61] do not affect our discussion and are, thus, dropped altogether). The potential $V(\phi)$ is assumed to contain part of the subcritical five-dimensional string theory contributions to the effective action. The metric background (in the Einstein frame) is written in the conformal gauge in the usual form

$$ds^2 = b(z)^2\left[f(z)d\tau^2 + d\vec{x}^2 + \frac{dz^2}{f(z)}\right], \tag{24}$$

while the dilaton is assumed to depend only upon the radial coordinate z, $\phi = \phi(z)$, and τ is a periodic coordinate with period $1/T$. Comparing with Eq. (11), one sees that $b(z) = e^{\mathcal{A}(z)}$. The Einstein and scalar equations of motion that follow from extremizing (23) are

$$\begin{gathered}\frac{f''}{f'} + 3\frac{b'}{b} = 0,\\ 6\frac{b'^2}{b^2} - 3\frac{b''}{b} = \frac{4}{3}\phi'^2 \quad \text{and}\\ 6\frac{b'^2}{b^2} + 3\frac{b''}{b} + 3\frac{b'}{b}\frac{f'}{f} = \frac{b^2}{f}V,\end{gathered} \tag{25}$$

where the prime indicates differentiation with respect to z. The equation of motion for ϕ is a combination of the previous equations—as usual for Einstein's equations, there is some redundancy in the equations of motion (due to Bianchi's identity).

B. Exact solution—model A

An analytical solution [33] of the equations of motion (25) is given by trying the ansatz

$$b(z) = \frac{R}{z}e^{-\frac{1}{3}\Lambda^2 z^2}, \tag{26}$$

where Λ is an infrared scale of the order of Λ_{QCD}. Defining the dimensionless variable $y \equiv \Lambda z$ and $\lambda = e^{\phi}$, one can integrate the equations of motion to find [37]

$$\frac{\lambda(y)}{\lambda_0} = \exp\left(\frac{\sqrt{\frac{9}{y^2}+4}\,y(2\sqrt{4y^2+9}\,y + 9\sinh^{-1}(\frac{2y}{3}))}{8\sqrt{4y^2+9}}\right), \tag{27}$$

where $\lambda_0 = \lambda(0)$. Also, the horizon function is given by

$$f(y, y_h) = 1 - \frac{(y^2-1)e^{y^2}+1}{1+e^{y_h^2}(y_h^2-1)}. \tag{28}$$

Finally, the dilaton potential for this solution is given by

$$\begin{aligned}V(y, y_h) = \frac{12}{R^2}e^{\frac{2y^2}{3}}\Bigg[&\left(\frac{1}{3}y^4 + \frac{5}{6}(y^2+1)\right)f(y, y_h)\\ &- \left(\frac{1}{2}+\frac{1}{3}y^2\right)\frac{y}{2}\frac{\partial f}{\partial y}(y, y_h)\Bigg].\end{aligned} \tag{29}$$

Note that the potential depends explicitly on the temperature via the position of the horizon y_h. This is not going to be the case in the other type of models considered in Sec. V.

1. Thermodynamics

The temperature of the thermal bath is given by the Hawking temperature of the black brane

$$T = \frac{|f'(z_h)|}{4\pi} = \frac{\Lambda}{2\pi}\frac{y_h^3}{y_h^2 - 1 + e^{-y_h^2}}. \tag{30}$$

The entropy density is given by the Bekenstein–Hawking formula, which yields

$$s = \frac{b(z_h)^3}{4G_5} = \frac{R^3\Lambda^3}{4G_5}\frac{e^{-y_h^2}}{y_h^3}. \tag{31}$$

Moreover, the pressure follows from $s = \partial p/\partial T$,

$$p(y_h) = -\int_{y_h}^{\infty} s(T(x))\frac{dT(x)}{dx}, \tag{32}$$

and the energy density is given by $\epsilon = sT - p$.

The temperature function $T(y_h)$ has a minimum for $T_{\mathrm{min}} = 0.396\Lambda$, $y_h^{\mathrm{min}} = 1.466$. For $T < T_{\mathrm{min}}$, there is no possible black brane solution, and the system is in a thermal gas phase. However, for $T_{\mathrm{min}} < T < T_c$, where $T_c = 0.400\Lambda$ is reached at $y_h^c = 1.299$, albeit there is a black brane solution, the pressure is negative—this signals that the thermal plasma is in a metastable phase. For $T > T_c$ (thus, $y_h < y_h^c$), we have a deconfined thermal plasma state. Since the entropy density has a discontinuity at $T = T_c$, the transition is of first order. It is possible to explicitly write the equation of state of the system in terms of the speed of sound squared:

$$c_s^2 = \frac{d\log T}{d\log s} = \frac{1}{3+y_h^2}\frac{3 - y_h^2 - (3+2y_h^2)e^{-y_h^2}}{y_h^2 - 1 + e^{-y_h^2}}. \tag{33}$$

In Fig. 2 we compare the equation of state of this model, given by (30) and (33), with lattice results for a pure glue SU(3) Yang–Mills plasma [42]. We see that this gravity dual provides a reasonable qualitative description of the equation of state of a pure glue plasma, more so considering its relative simplicity and the fact that it is an analytical solution of the Einstein + scalar equations of motion. However, it must be noted that this simple realization of

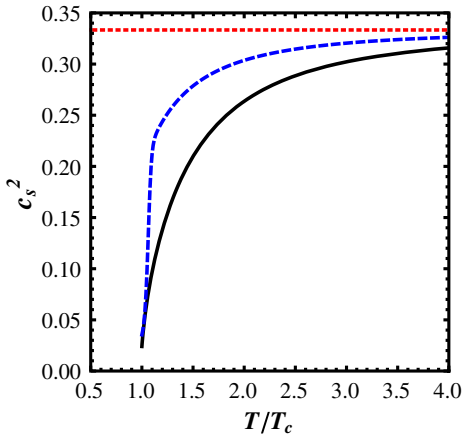

FIG. 2 (color online). Speed of sound squared c_s^2 of the plasma as a function of T/T_c, where T_c denotes the critical temperature for a deconfining first-order transition. The solid black line is the result for the particular IHQCD model studied (see Sec. IV B), the dashed blue line corresponds to lattice results from Ref. [42] for an SU(3) Yang–Mills plasma, while the horizontal red line gives the result for a conformal plasma, $c_s^2 = 1/3$.

IHQCD does not describe lattice data quantitatively between $T/T_c = 1.1$–2.5.[3]

2. Polyakov loop

An interesting quantity to compute in this nonconformal model is the expectation value of the Polyakov-loop operator [62–65]

$$\hat{L}(\vec{x}) = \frac{1}{N_c}\mathrm{Tr}P\exp\left(i\int_0^\beta \hat{A}_0(\tau,\vec{x})d\tau\right), \tag{34}$$

where P indicates path ordering and the trace is in the fundamental representation. Holographically, the evaluation of the Polyakov loop in a thermal gauge theory in the imaginary time formalism corresponds to calculating the classical worldsheet action for a *straight* string in the bulk stretching from the conformal boundary to the horizon. This string worldsheet wraps the imaginary time circle S^1 (for details of the holographic computation of the Polyakov and Wilson loops in this context, see Refs. [52,66–71]). At strong coupling and large N_c, the norm of the expectation value of the Polyakov-loop operator (34) is given by

$$|\langle\hat{L}\rangle| \sim e^{-F_Q/T} \sim e^{-S_{\mathrm{NG}}}, \tag{35}$$

where F_Q is the difference in the free energy of the thermal bath due to the inclusion of a single probe heavy quark in the system, and S_{NG} is the (Euclidean) Nambu–Goto action for the string worldsheet,

$$S_{\mathrm{NG}} = \frac{1}{2\pi\alpha'}\int d^2\sigma\sqrt{\det\left(g^s_{\mu\nu}X^\mu_a X^\nu_b\right)}, \tag{36}$$

where $\alpha' = \ell_s^2$, ℓ_s is the string length, X^μ_a are the embedding functions of the string worldsheet in the target space-time, and $g^s_{\mu\nu}$ is the metric in the string frame—since this background comes from a five-dimensional noncritical string theory, $g^s_{\mu\nu} = \lambda^{4/3}g_{\mu\nu}$, where $g_{\mu\nu}$ is the metric in the Einstein frame [32,33]. The indices $\mu,\nu = 0,1,2,3,4$ are space-time indices, and $a,b = \sigma,\tau$ are indices for the string worldsheet coordinates. Evaluating the worldsheet specified above with the background (24), one can see that

$$F_Q = \frac{1}{2\pi\alpha'}\int_0^{y_h} dy\sqrt{g_{00}g_{zz}} = \frac{1}{2\pi\alpha'}\int_0^{y_h} dy b_s^2(y), \tag{37}$$

where $b_s \equiv \lambda^{2/3}b$. As expected, the bare heavy quark free energy is UV divergent and must be regularized. To regularize it, we use a temperature independent subtraction,

$$\bar{F}_Q = \frac{1}{2\pi\alpha'}\int_0^{y_h^c} dy(b_s^{(0)}(y))^2, \tag{38}$$

where $b_s^{(0)}(y)$ is the vacuum form of $b_s(y)$. The regularized free energy is then $F_Q^{\mathrm{reg}} = F_Q - \bar{F}_Q$. For the geometry in question,

$$\frac{F_Q^{\mathrm{reg}}T_c}{\sigma} = -\frac{T_c}{\Lambda b_s^2(y_{\mathrm{min}})}\int_{y_h}^{y_h^c} dy b_s^2(y), \tag{39}$$

where, to facilitate the comparison with lattice results, we normalized the heavy quark free energy by the holographically computed string tension σ (associated with the area law for the rectangular Wilson loop in the vacuum) and by the critical temperature T_c. The holographic string tension in IHQCD is generally given by $\sigma = R^2\Lambda^2 b_s^2(y_{\mathrm{min}})/(2\pi\alpha')$ [33], where y_{min} denotes the location of the minimum of the U-shaped Nambu–Goto string profile in the bulk used in the calculation of the rectangular Wilson loop for asymptotically large separations.

Note that the Polyakov loop computed on the lattice depends on the choice of renormalization scheme since the heavy quark bare free energy is divergent in the continuum limit (one needs to subtract the divergent part and fix the renormalization constant). In the calculations of Ref. [53], this constant term was set to zero. Clearly, any other value for the constant would be fine, and the scheme dependence just corresponds to adding an additive constant in the free energy of the renormalized Polyakov loop.[4] In this

[3]This can be remedied by choosing an appropriate dilaton potential, and, as shown in Refs. [32–36], a good quantitative agreement with pure glue lattice QCD thermodynamics in this temperature range can be achieved.

[4]We thank M. Panero for discussions about this point.

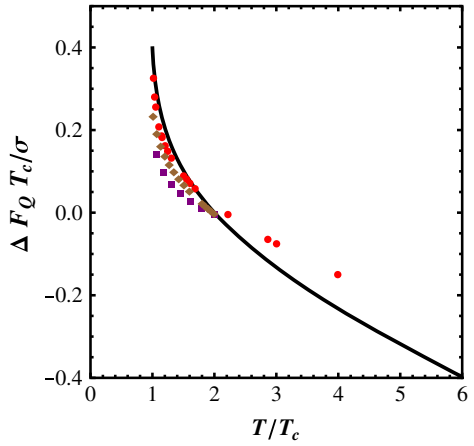

FIG. 3 (color online). $\Delta F_Q T_c/\sigma = (F_Q(T) - F_Q(2T_c))T_c/\sigma$ as a function of T/T_c for model A (solid black line) defined in Sec. IV B and for SU(N_c) Yang–Mills [53] with $N_c = 3$ red circles), 4 (purple squares), and 5 (brown diamonds).

paper we chose to compare the free energy difference $\Delta F_Q T_c/\sigma = (F_Q(T) - F_Q(2T_c))T_c/\sigma$ as a function of T/T_c computed in the model with the one found on the lattice (note that this still corresponds to choosing a scheme in which the free energy difference vanishes at $2T_c$).

We compare in Fig. 3 the holographic result (39) with the lattice results for the SU(N_c) Yang–Mills lattice data with a different number of colors from Ref. [53]. One can see that, even though the thermodynamics of the simple IHQCD model only reproduces qualitatively the lattice data, the holographic result for F_Q gives a reasonable description of the lattice data for $T_c < T < 2T_c$. Moreover, even though holographic models ought to be valid only for large N_c, reasonable agreement is seen even for $N_c = 3$.

3. Debye screening mass

Let us begin by studying the bulk axion spectrum at $T = 0$ (i.e., we set $f = 1$). The first step is to discuss the function $\mathcal{Z}$ in the action for the axion fluctuations (10), which represents a partial resummation of higher-order forms coming from five-dimensional subcritical string theory [32,33]. In the UV, $Z(\lambda) \sim$ const, while in the IR $(\lambda) \propto \lambda^4$ to ensure glueball universality. We will use the standard IHQCD parametrization that interpolates between these two cases [54],

$$Z(\lambda) = c_0 + c_4\lambda^4, \tag{40}$$

where c_0 and c_4 are constants. By a suitable normalization of the action, one can set $c_0 = 1$. To study the dependence of the results with c_4, we choose three values for it spanning a large range of values for this coefficient: 0.1, 1, and 10.

The numerical procedure to find the spectrum is the same as the one described in Sec. III. For the vacuum case, we consider the Schrödinger equation (16) and the asymptotic potential in the UV, including the first subleading correction in $1/y$, which gives

$$\mathcal{V}(y) = \frac{15}{4y^2} - \frac{9\sqrt{2}c_4}{(1+c_4)y} + \mathcal{O}(1). \tag{41}$$

The asymptotic equation (including the subleading term) can be solved analytically and the linearly independent solutions are Whittaker functions $M_{\kappa,\mu}$ and $W_{\kappa,\mu}$ [72]. If we consider only the leading term in $1/y$, these solutions reduce to the Bessel functions found in Sec. III. The normalized near boundary series expansion, including the subleading term in (41), is given by

$$\psi(y) = y^{1/2}\left(y - \frac{9\sqrt{2}c_4}{5}\frac{y^2}{1+c_4} + \cdots\right). \tag{42}$$

Using the shooting method to solve the eigenvalue problem, we obtain the results shown in Table I. One can see that glueball mass associated with the bulk axion in the vacuum is quite insensitive to the choice of c_4 and $m_{J^{PC}=0^{-+}} \sim 3\Lambda$. This value is also comparable with the corresponding results for the lightest $J^{PC} = 0^{++}$ and $J^{PC} = 2^{++}$ glueballs in this model, $m_{J^{PC}=0^{++}} \approx 2.5\Lambda$ and $m_{J^{PC}=2^{++}} = \sqrt{8}\Lambda \sim 2.2\Lambda$ [37].

Let us now proceed to extract the Debye screening mass in this model. Consider now the background at nonzero temperature. The equation of motion to solve is now of the form (15). The asymptotic solution is the same as in the $T = 0$ case since $f \to 1$ for $y \to 0$. We use the same choices for c_4 employed in the preceding calculation. Our results can be found in Fig. 4. Since at high temperatures $T \gg \Lambda$ the geometry of the gravity dual simplifies to AdS_5, one must have $m_D(T \gg \lambda) \to c\pi T$ with $c = 3.4041$ as shown in Sec. III. Thus, our results for m_D are normalized by $c\pi T$.

One can see that the results are somewhat insensitive to the choice of c_4 as long as $c_4 \gtrsim 1$. Also, we note that for $T \to T_c^+$, $m_D/(c\pi T) \sim 0.18$, which is nearly independent of c_4—the Debye mass has a discontinuity at $T = T_c$. As expected, for increasing temperature, the plasma becomes more and more screened—m_D is monotonically increasing with T until it reaches its conformal value.

Reference [24] computed the thermal screening lengths for an $\mathcal{N} = 2^*$ plasma, which is nonconformal deformation

TABLE I. Glueball mass $m_{J^{PC}=0^{-+}}$ associated with the bulk axion at $T = 0$ for some choices of c_4 computed using the model in Sec. IV B.

c_4	m_{axion}/Λ
0.1	3.0433
1.0	2.996
10.0	2.986

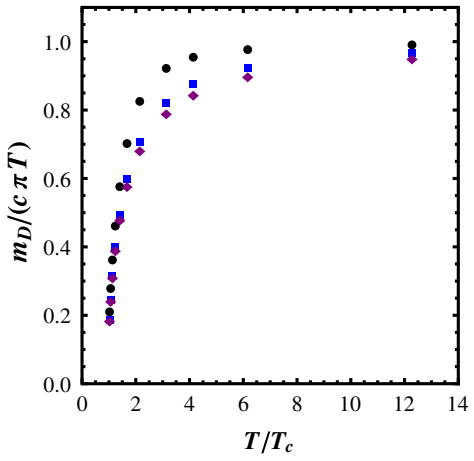

FIG. 4 (color online). Debye screening mass m_D for the simplified IHQCD model discussed in Sec. IV B, normalized by the $\mathcal{N}=4$ SYM Debye mass at strong coupling $c\pi T$ with $c=3.4041$. We present the results for $c_4=0.1$ black circles), 1 (blue squares), and 10 (purple diamonds).

of the $\mathcal{N}=4$ SYM plasma obtained by giving a mass μ to the adjoint scalars and fermions [73–75]. Using this top-down nonconformal construction [24] also obtained that m_D/T (computed from the axion fluctuations) becomes smaller than its conformal value at low temperatures when $\mu/T>1$. However, this theory does not possess a finite temperature phase transition, and, thus, the discontinuity in m_D/T at T_c found here is a new feature brought in by the nonconformal plasmas constructed within IHQCD.

V. B CLASS OF MODELS—OVERVIEW

In this section we shall describe a second class (model B) of strongly coupled non-Abelian plasmas with gravity duals described by Einsten + scalar actions [38–40] (see also Refs. [69,70,76]) built in order to reproduce some of the thermodynamic results obtained on the lattice at zero baryon chemical potential. Even though the bulk fields are the same as in the previous section, in these models the scalar field corresponds to a relevant operator in the UV.

The interpretation put forward in Ref. [39] is that, since these gravity models cannot truly describe perturbative QCD physics in the UV, one must choose an intermediate semihard scale at which asymptotic freedom is replaced by conformal invariance. In fact, given that the scaling dimension Δ of the glueball operator $\mathrm{Tr}F^2$ is not a protected quantity in QCD and it becomes smaller than 4 toward the IR, this semihard scale may be used to define the range of applicability of this effective holographic model in this context. This implies that, in general, these models should not be used at high temperatures where asymptotic freedom becomes dominant. However, as shown in Ref. [76], these nonconformal bottom-up models are able to describe not only the equilibrium quantities found on the lattice but also the temperature dependence of some nontrivial transport coefficients such as the electrical conductivity recently computed on the lattice [77]. Moreover, these models also give valuable insight into the energy loss experienced by heavy (and also light quarks) in the QGP near the crossover phase transition [78–80]. Therefore, we believe that it is relevant to consider these constructions here as well and investigate the temperature dependence of m_D/T in these models. We shall see that by carefully choosing the scalar potential one can obtain a much better quantitative description of the thermodynamics of pure glue as well as that of QCD with light dynamical flavors found on the lattice.[5]

A. Bulk action

Even though the bulk action that defines these models is the same as that studied in Sec. IV, we find it convenient to follow the convention of Ref. [38] [compare the dilaton normalization in Eq. (23) with the one below] where the Einstein + scalar action is

$$S=\frac{1}{2\kappa_5^2}\int d^5x\sqrt{g}\left[\mathcal{R}-\frac{1}{2}(\partial_\mu\phi)(\partial^\mu\phi)-V(\phi)\right], \quad (43)$$

where $k_5^2=8\pi G_5$. The scalar field in this action is related to the dilaton in model A (23) by a factor of $\sqrt{3/8}$. The potential $V(\phi)$ is chosen in such a way that the thermodynamic properties of the model (43) mimic the ones desired from the gauge theory—in the next subsections, we will describe simple choices of $V(\phi)$ which achieve this task. The desired solutions of Eq. (43) must be asymptotically AdS_5 for the boundary gauge theory to have a UV fixed point. The potential $V(\phi)$ is chosen in order to interpolate between a free massive scalar field (plus cosmological constant term) near the boundary, $V(\phi)\sim -12/R^2+m^2\phi^2/2$, and a potential which yields the Chamblin–Reall solution [84] deep in the bulk, $V(\phi)=V_0e^{\gamma\phi}$, with $\gamma<0$.

B. Metric ansatz

As we wish to study the gauge theory at finite temperature, the solution also must contain a black brane in the bulk. We also want translation symmetry in the gauge theory and rotational SO(3) symmetry in the spatial directions but not the full Lorentz SO(3, 1) symmetry since the at nonzero temperature the thermal gauge theory is not invariant by Lorentz boosts. An ansatz which is able to satisfy these requirements, called here the Gubser gauge [38], is

[5]We note that the models considered here do not have the correct bulk degrees of freedom to fully describe the physics associated with chiral symmetry breaking. See Refs. [81,82] for a model which describes chiral symmetry breaking in this class of Einstein + scalar models by including a second scalar field, following the spirit of the Karch-Katz-Son-Stephanov (KKSS) model [83].

$$ds^2 = e^{2A}(hd\tau^2 + d\vec{x}^2) + e^{2B}\frac{d\phi^2}{h}, \tag{44}$$

where the holographic radial coordinate is given by the scalar field ϕ itself. We require that A, B, and h are only functions of ϕ, i.e., $A(\phi)$, $B(\phi)$, and $h(\phi)$. The asymptotically AdS_5 boundary is recovered when $\phi \to 0$. This choice, as shown in Ref. [38], is convenient to solve the equations of motion for the action (43). However, this gauge choice is not very useful for analyzing the glueball spectra or studying Wilson and Polyakov loops. For these purposes, it is convenient to go back to conformal gauge. We discuss this point in more detail in Appendix A.

C. Equations of motion—general case

It is possible to write a "master" equation that yields all the metric functions in the ansatz (44) in terms of a single ordinary first-order differential equation [38]. The equations of motion derived from the action (43) are Einstein's equations

$$\mathcal{R}_{\mu\nu} - \frac{g_{\mu\nu}}{2}\mathcal{R} = 8\pi G_5 T_{\mu\nu}, \tag{45}$$

where $T_{\mu\nu}$ is the stress-energy tensor for the scalar field. The equation of motion for the scalar field ϕ is

$$\nabla_\mu \nabla^\mu \phi - V' = 0, \tag{46}$$

where ∇ indicates the covariant derivative and $V' = dV/d\phi$ (in this section, primes will always indicate derivatives with respect to ϕ). With the ansatz (44), one can see that the equation of motion for the $\tau\tau$ component is

$$2e^{2B}V + 6A'h' + h(24A'^2 - 12B'A' + 12A'' + 1) = 0, \tag{47}$$

while for the xx the equation of motion is

$$2e^{2B}V + 14A'h' - 2B'h' + 2h'' + h(24A'^2 - 12B'A' + 12A'' + 1) = 0. \tag{48}$$

The common term in parentheses can be eliminated from both equations, which yields

$$h'' + (4A' - B')h' = 0. \tag{49}$$

The $G_{\phi\phi}$ equation of motion is

$$6A'h' + h(24A'^2 - 1) + 2Ve^{2B} = 0. \tag{50}$$

Using the $G_{\tau\tau}$ equation of motion (47) to eliminate $24A'^2$ from Eq. (47), we obtain

$$A'' - A'B' + \frac{1}{6} = 0. \tag{51}$$

The last equation of motion is given by the scalar equation (46),

$$(4A' - B') + \frac{h'}{h} - \frac{e^{2B}}{h}V' = 0. \tag{52}$$

We use the set consisting of Eqs. (49) to (52) as our equations of motion. These equations are not completely independent due to Bianchi's identity. In this case, the derivative of Eq. (51) follows from the derivative of the other equations of motion, and one can use any subset of three equations among these to obtain the full geometry.

D. Zero temperature master equation

We start by describing zero temperature solutions. With a vacuum solution at hand, one can proceed to explore the properties of the $T = 0$ strongly coupled non-Abelian gauge theory with gravity dual given by Eq. (43). Although this class of models was built primarily in order to reproduce the thermodynamics of QCD near the crossover phase transition [85], in Appendix B we show that the glueball spectra are reasonably described by a confining, zero temperature version of these models.

When $T = 0$, the boundary gauge theory has full Lorentz invariance, and, thus, we set $h = 1$ in (44)

$$ds^2 = e^{2A}(d\tau^2 + d\vec{x}^2) + e^{2B}d\phi^2, \tag{53}$$

where τ is the Euclidean time. The equation of motion (49) is identically satisfied when $h = 1$. The remaining equations of motion (50), (51), and (52) simplify to

$$A'' - A'B' + \frac{1}{6} = 0, \tag{54}$$

$$24(A')^2 - 1 + 2e^{2B}V = 0 \quad \text{and} \tag{55}$$

$$4A' - B' - e^{2B}V' = 0. \tag{56}$$

Now, following the procedure used in Ref. [38] for the $T \neq 0$ case, our goal here is to obtain a first-order master equation for $G(\phi) \equiv A'(\phi)$. Then, one can integrate G to obtain A and the remaining metric function B. Combining Eqs. (55) and (56), we arrive at

$$\frac{V}{V'} = \frac{-8G + 2B'}{24G^2 - 1}. \tag{57}$$

We can now use Eq. (54) to eliminate B' from this equation and find the master equation at $T = 0$,

$$G + \frac{V}{3V'} = -\frac{6G'G}{24G^2 - 6G' - 1}. \tag{58}$$

This is a first-order ordinary differential equation for $G = A'$ for a given potential $V(\phi)$. To solve it, we have to specify a boundary condition for $G(\phi)$. Since all the potentials we shall consider have the IR ($\phi \to \infty$) asymptotic $V(\phi) \propto e^{\gamma\phi}$, we see that for $\phi \to \infty$, $V/3V' = 1/(3\gamma)$. Thus, Eq. (58) implies that when $\phi \to \infty$ one must have

$$G(\phi \to \infty) = -\frac{1}{3\gamma}. \tag{59}$$

E. Finite temperature master equation

The procedure for extracting a master equation for the finite temperature case was explained in detail in Ref. [38], and we shall not repeat it here. One can show that this master equation is

$$\frac{G'}{G+\frac{V}{3V'}} = \frac{d}{d\phi}\log\left[\frac{G'}{G} + \frac{1}{6G} - 4G - \frac{G'}{G+\frac{V}{3V'}}\right]. \tag{60}$$

Let us now discuss the boundary conditions for the master equation (60). First, we require that $h(\phi)$ has a simple zero at $\phi = \phi_h$, which is the radial position of the event horizon. Thus, $h(\phi_h) = 0$ but $h'(\phi_0) \neq 0$ so that for $\phi \lesssim \phi_h$, $h(\phi) \approx -h'(\phi_h)(\phi - \phi_h)$. Therefore, from Eqs. (50) and (51), one obtains the constraints

$$V(\phi_h) = -3e^{-2B(\phi_h)}G(\phi_h)h'(\phi_h) \quad \text{and} \tag{61}$$

$$V'(\phi_h) = e^{-2B(\phi_h)}h'(\phi_h). \tag{62}$$

Thus, near the horizon one may expand $G + V/(3V')$ in a series around $\phi = \phi_h$,

$$G(\phi) = -\frac{1}{3}\frac{V(\phi_h}{V'(\phi_h)} + \frac{1}{6}\left(\frac{V(\phi_h)V'(\phi_h)}{V'(\phi_h)^2} - 1\right)(\phi - \phi_h) + O[(\phi - \phi_h)^2]. \tag{63}$$

By fixing the position of the horizon ϕ_h, we may use the series solution (63) to obtain $G(\phi)$ near the horizon, at $\tilde{\phi} = \phi_h - \delta\phi$, for $\delta\phi \ll \phi_h$, and then integrate numerically from $\phi = \tilde{\phi}$ out to $\phi = 0$ using the series values for $G(\tilde{\phi})$ and $G'(\tilde{\phi})$ as boundary conditions.

F. Geometry asymptotics

As mentioned above, the potential near the boundary ($\phi \to 0$) is given by

$$V(\phi) \sim -\frac{12}{R^2} + \frac{m^2}{2}\phi^2. \tag{64}$$

The UV scaling dimension Δ of the gauge theory operator associated with ϕ is determined by the larger root of

$$\Delta(\Delta - 4) = m^2R^2. \tag{65}$$

In the coordinate system (44), the asymptotic AdS_5 geometry ($\phi \to 0$) is given by

$$A(\phi) = \frac{\log\phi}{\Delta - 4} + O(1) \text{ and} \tag{66}$$

$$B(\phi) = -\log\phi + O(1), \tag{67}$$

with $h(\phi \to 0) \to 1$. This also fixes the asymptotic behavior $G(\phi \to 0) \sim 1/(\phi(\Delta - 4))$.

G. Obtaining the geometry and the thermodynamics

With the boundary conditions fixed and with the asymptotic behavior defined above, one can obtain the full metric from $G(\phi)$. First, one can see that

$$A(\phi) = A_h + \int_{\phi_h}^{\phi} d\tilde{\phi}G(\tilde{\phi}), \tag{68}$$

where $A_h = A(\phi_h)$ is the integration constant. Since near the boundary A behaves as in Eq. (66), one can obtain the integration constant A_h,

$$A_h = \frac{\log\phi_h}{\Delta - 4} + \int_0^{\phi_h} d\phi\left[G(\phi) - \frac{1}{(\Delta - 4)\phi}\right]. \tag{69}$$

Now, let us also evaluate $B(\phi)$ and $h(\phi)$. One can solve Eq. (51) for B' in terms of G to obtain

$$B(\phi) = B_h + \int_0^{\phi_h} d\phi\left[\frac{G'(\phi)}{G(\phi)} + \frac{1}{6G(\phi)}\right], \tag{70}$$

with $B_h = B(\phi_h)$ being an integration constant, which we will determine in the end of this subsection. Also, given that A and B are known, one can integrate Eq. (49) to obtain

$$h(\phi) = h_0 + h_1\int_{\phi_h}^{\phi} d\tilde{\phi}e^{-4A(\tilde{\phi})+B(\tilde{\phi})}, \tag{71}$$

where h_0 and h_1 are integration constants. To determine them, remember that $h(\phi \to 0) = 1$ and $h(\phi_h) = 0$ so that

$$h_0 = 0 \quad \text{and} \quad h_1 = \frac{1}{\int_{\phi_h}^{0} d\phi e^{-4A(\phi)+B(\phi)}}. \tag{72}$$

One can show that the Hawking temperature is

$$T = \frac{e^{A_h+B_h}|V_h'|}{4\pi}, \tag{73}$$

and this can be shown to be [38]

$$T = \frac{\phi_h^{1/(\Delta-4)}}{\pi R}\frac{V(\phi_h)}{V(0)} \times \exp\left\{\int_0^{\phi_h}\left[G(\phi) - \frac{1}{(\Delta-4)\phi} + \frac{1}{6G(\phi)}\right]\right\}, \quad (74)$$

where we used that $V(\phi \to 0) \to -12/R^2$, to leading order in ϕ. Moreover, one can also find

$$B_h = \log\left[\frac{4V(\phi_h)}{V(0)V'(\phi_h)L}\right] + \int_0^{\phi_h}\frac{d\phi}{6G(\phi)}. \quad (75)$$

Let us continue with the thermodynamics. As Eq. (43) is just the Einstein–Hilbert action coupled with some matter fields, the entropy density of the black brane is given by the area of the horizon

$$s = \frac{2\pi}{k_5^2}e^{3A(\phi_h)}. \quad (76)$$

Therefore, Eqs. (74) and (76) give a thermodynamical equation of state parametrized by ϕ_h: $(T(\phi_h), s(\phi_h))$. In particular, one can write the equation of state in terms the speed of sound:

$$c_s^2 = \frac{d\log T}{d\log s} = \frac{d\log T/d\phi_h}{d\log s/d\phi_h}. \quad (77)$$

H. Choice of the scalar potential

In this framework, the potential $V(\phi)$ is chosen to match the QCD plasma thermodynamics at zero chemical potential. As mentioned above, the main restrictions on $V(\phi)$ are that near the boundary $\phi \to 0$, $V(\phi) \sim -12/R^2 + m^2\phi^2/2$, while near the black brane horizon, $V(\phi) \sim V_0 e^{\gamma\phi}$. A simple, fairly featureless, potential that satisfies both conditions is

$$V(\phi) = -\frac{12}{R^2}(1 + a\phi^4)^{1/4}\cosh(\gamma\phi) + b_2\phi^2 + b_4\phi^4 + b_6\phi^6, \quad (78)$$

where γ, b_2, b_4, and b_6 are the free parameters of the potential.[6]

The parameter a controls the nature of the thermodynamical phase transition; as we shall see, $a = 1$ implies that the bulk theory has a Hawking–Page transition, and thus the dual gauge theory has a first-order phase transition—this class of models can be used to mimic the properties of the deconfinement transition in SU(N_c) Yang–Mills theory [41,42]. On the other hand, $a = 0$ implies that the dual gauge theory has a crossover phase transition, and the model can be used to describe the thermodynamics of QCD with $(2+1)$ light quark flavors [44]. The models with $a = 1$ and $a = 0$ will be called here B1 models and B2 models, respectively.

[6]Reference [86] obtained an important constraint that must be obeyed in order to avoid naked singularities that cannot be covered by a black brane horizon at finite temperature: $V(0) \geq V(\phi)$ for $\phi \neq 0$. For the choices of scalar potentials used here, within the range in temperature we were interested in, we did not find any naked singularities that could not be covered by a horizon.

TABLE II. Parameters for the B1 (first-order phase transition) and B2 (crossover phase transition) models. The last column shows the corresponding scaling dimension Δ of each model.

	a	γ	b_2	b_4	b_6	Δ
Model B1	1	$\sqrt{2/3}$	5.5	0.3957	0.0135	3.0
Model B2	0	0.606	0.703	-0.12	0.0044	3.0

The near-UV ($\phi \to 0$) mass m^2 of the bulk effective action can be extracted from Eq. (78):

$$m^2 = -\frac{12\gamma^2}{R^2} + 2b_2. \quad (79)$$

On the other hand, as in the UV Eq. (65) holds, one obtains that b_2, Δ, and γ are not independent,

$$b = \frac{6\gamma^2}{R^2} + \frac{\Delta(\Delta-4)}{2R^2}. \quad (80)$$

In Table II we show the parameters for both models we consider in this work. We remark that in both models $\Delta = 3$, as used before in Refs. [78–80]. These two sets of parameters were chosen in order to fit lattice data for pure SU(3) Yang–Mills theory and QCD, respectively—we shall display the numerical results for the thermodynamics in the corresponding sections for each model.

VI. DEBYE SCREENING MASS AND POLYAKOV LOOP IN THE B1 MODEL

Let us start by the B1 model which possesses a first-order deconfining phase transition and models the thermodynamics of pure SU(N_c) Yang–Mills theory.

A. Thermodynamics

To obtain the thermodynamics of this model, we use Eqs. (74) and (76). We start by presenting, in Fig. 5, the temperature T (normalized by the critical temperature T_c for the first-order transition) as a function of ϕ_h. As in model A, we have two characteristic temperatures. First, we have a minimum temperature $T_{\rm min}$ (given by the minimum of T in Fig. 5) below which the black hole solution does not exist and the dominating bulk geometry corresponds to a thermal gas. The second distinctive temperature is the critical temperature, T_c, at which the pressure of the black

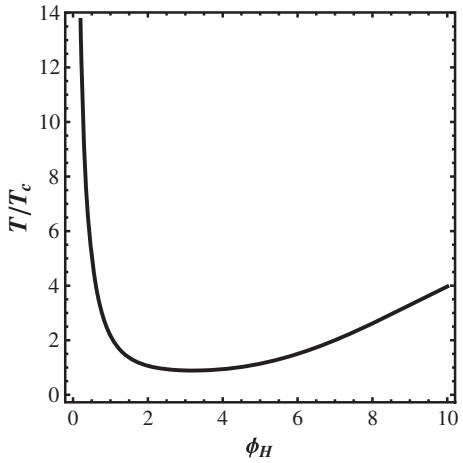

FIG. 5. Temperature T (normalized by the critical temperature T_c) as a function of the horizon position in the holographic coordinate ϕ_h for the B1 model.

brane solution vanishes. For temperatures T such that $T_{\rm min} < T < T_c$, the thermal plasma is in a (superheated) metastable phase. For the parameters we used, given in Table II, $T_{\rm min} = 0.89T_c$, with $\phi_{h,\rm min} = 3.20$ and $\phi_{h,c} = 2.20$.

From Eq. (76) we evaluate the entropy density s as a function of ϕ_h. Using the results shown in Fig. 5, one can eliminate ϕ_h and obtain s as a function of T. With $s(T)$, one may proceed to evaluate all the thermodynamic functions. For instance, the pressure p is given by

$$p = -\int_{\infty}^{\phi_h} s(x)T'(x)dx, \tag{81}$$

while c_s^2 is given by Eq. (77). In Fig. 6 we show the pressure p (normalized by the $\mathcal{N} = 4$ SYM result) as a function of T/T_c. In Fig. 7, we compare the model results for the equation of state written in terms of c_s^2 with the

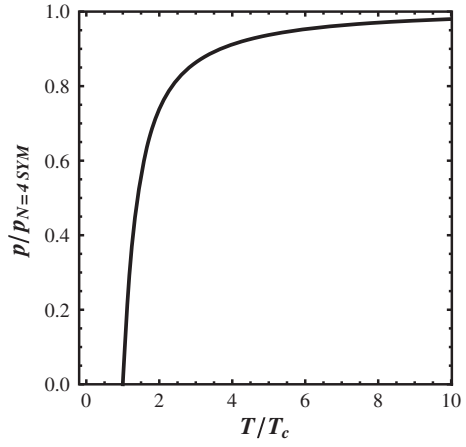

FIG. 6. The pressure p of the plasma for model B1, normalized by the $\mathcal{N} = 4$ SYM result, as a function of the normalized temperature T/T_c.

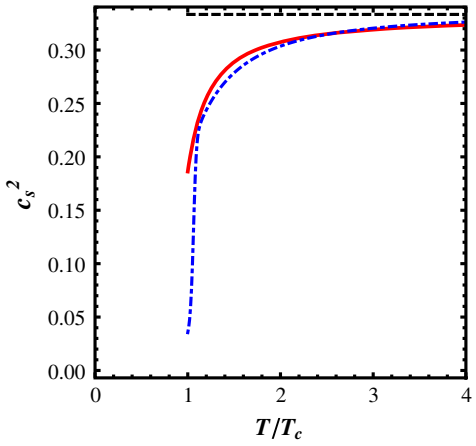

FIG. 7 (color online). The speed of sound squared of the plasma c_s^2 for model B1 as a function of the normalized temperature T/T_c (solid red curve), compared with SU(3) Yang–Mills lattice results (dot-dashed blue curve) [41]. The black dashed line is the conformal field theory (CFT) result, $c_s^2 = 1/3$.

corresponding lattice results for pure SU(3) Yang–Mills [41]. We see that the B1 model is in fair agreement with SU(3) thermodynamics representing a quantitative improvement with respect to model A.

B. Polyakov loop

The computation of the expectation value of the Polyakov loop proceeds as in Sec. IV B 2 using Eq. (39). This equation assumes that the geometry is in the conformal gauge; however, our numerical solution is obtained in the $\phi = z$ gauge. Thus, we need to perform a coordinate system change—the details of this gauge change can be found in Appendix A. Also, our geometry is given in the Einstein frame; to evaluate the Polyakov loop, we have used the string frame. As in model A, we assume that our geometry is related to some five-dimensional subcritical string theory and the string frame metric is related to the Einstein frame metric by $g^s_{\mu\nu} = \lambda^{4/3} g_{\mu\nu}$, where $\lambda = e^{\phi}$. A final remark is that in this model $b(y) \neq b_{(0)}(y)$ so that the cancelation that took place in model A does not happen in this case. The regularized expression for the heavy quark free energy is

$$\frac{F_Q^{\rm reg} T_c}{\sigma} = \frac{T_c}{\Lambda b_s^2(y_{\rm min})} \int_0^{y_h^c} dy (b_s^2(y) - b_{(0),s}^2(y)) - \frac{T_c}{\Lambda b_s^2(y_{\rm min})} \int_{y_h}^{y_h^c} dy b_s^2(y), \tag{82}$$

where $y = \phi$ in order to maintain the same notation used in (39). In Fig. 8 we show our numerical results for $\Delta F_Q \equiv F_Q(T) - F_Q(2T_c)$, comparing with lattice results for SU(N_c) [53]. One can see that model B1 follows more

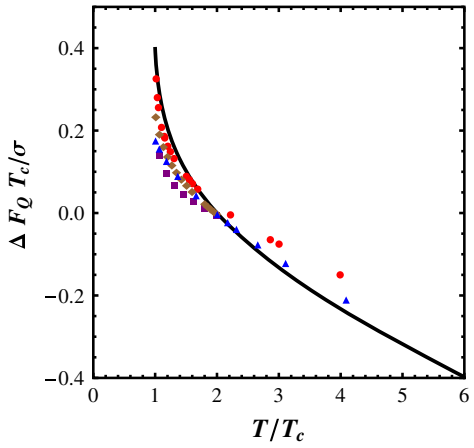

FIG. 8 (color online). $\Delta F_Q T_c/\sigma = (F_Q(T) - F_Q(2T_c))T_c/\sigma$ as a function of T/T_c for the model A (solid black line), model B1 (blue triangles), and for SU(N_c) Yang–Mills [53] with $N_c =$ 3 (red circles), 4 (purple squares), and 5 (brown diamonds).

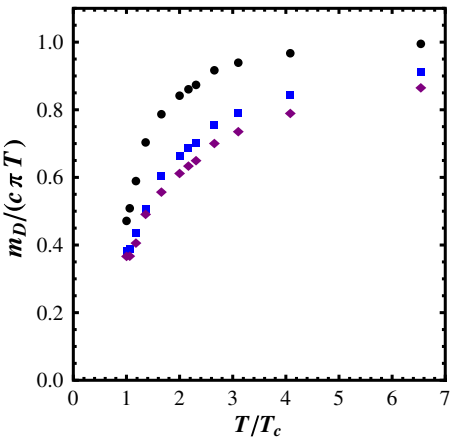

FIG. 9 (color online). Debye screening mass for the model B1, normalized by the $\mathcal{N} = 4$ SYM result $c\pi T$ (with $c = 3.4041$) as a function of T/T_c for $c_4 = 0.1$ (black circles), 1 (blue squares), and 10 (purple diamonds).

closely the lattice data in comparison that found for model A.[7]

C. Debye screening mass

We may now proceed to evaluate the Debye screening mass in model B1. To obtain the Debye mass, we have to obtain the lowest eigenvalue M^2 of the corresponding Eq. (15). As in the preceding subsection, this equation was written in the conformal gauge, whereas our numerical solution for the metric is obtained in the Gubser gauge. The numerical procedure to find m_D is exactly the same as described in Sec. IV B 3. As in model A, we assume that the axion action is given by Eq. (10), with the $\mathcal{Z}$ function given by the parametrization (40). We use the same values of c_4 as in the study of model A, $c_4 = 0.1, 1,$ and 10.

The numerical results for the Debye screening mass in this model are presented in Fig. 9. As in the case of model A, m_D/T has a discontinuity at $T = T_c$ where it jumps from 0 to a finite value $m_D/(c\pi T) \sim 0.35$ (somewhat higher than the jump in model A to $m_D/(c\pi T) \sim 0.2$). The value of the jump is not sensitive to the choice of c_4, and the overall behavior of m_D/T as a function of T saturates for large c_4. Note that we vary c_4 by 2 orders of magnitude, and m_D/T varies only by $\sim 20\%$ at high temperatures.

[7]It should be noted that our models are built to study phenomena near the confinement/deconfinement transition from $T \sim T_c = 150$ to $T \sim 3$–$4T_c \sim 450$–600 MeV. By construction, these models are strongly coupled in the UV. A reflection of this fact is that one cannot describe adequately both the Polyakov loop and the thermodynamics simultaneously at high temperatures, near the conformal regime, as argued in Ref. [87].

VII. DEBYE SCREENING MASS IN THE B2 MODEL

A. Thermodynamics

In this section we describe a choice of scalar potential that yields an equation of state for the holographic strongly coupled plasma that closely matches the lattice results for $(2 + 1)$ QCD [44]. The parameters for this potential can be found in Table II. For this model, the black brane solution always dominates over the thermal gas solution; thus, there is no metastable phase and no $T_{\rm min}$. Also, there is no confinement at $T = 0$. Moreover, the temperature T as a function of ϕ_h is monotonically decreasing, as it can be seen in Fig. 10. The pressure of the black brane phase is always positive, and, thus, one cannot define a critical temperature T_c as in models A and B1. The phase transition in model B2 is of crossover type; the thermodynamic quantities and their derivatives of all orders are continuous across the "phase transition." In fact, the phase transition is

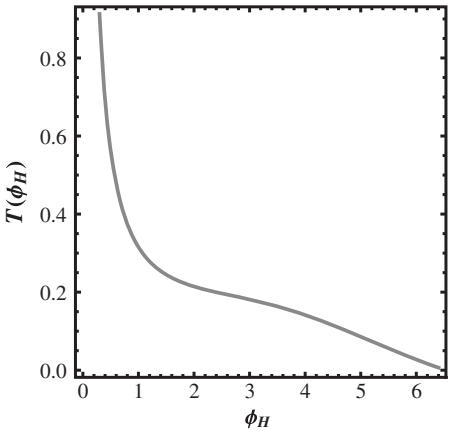

FIG. 10. Temperature T as a function of the horizon position in the holographic coordinate ϕ_h for model B2.

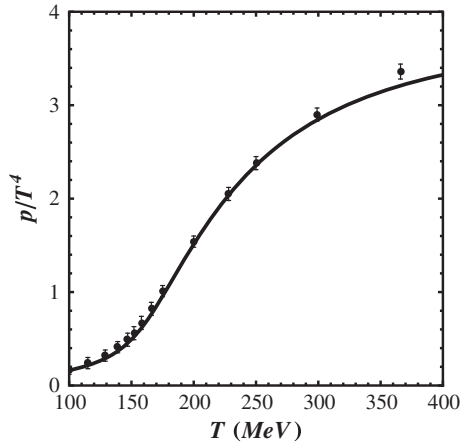

FIG. 11. The pressure of the plasma p/T^4 as a function of the normalized temperature T, for the B2 model (solid curve), compared with $(2+1)$ flavors SU(3) QCD lattice results (data points) [44].

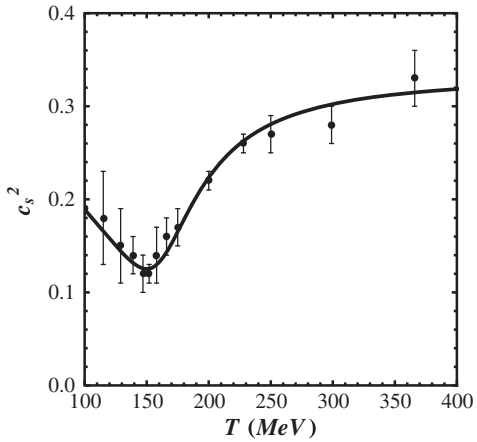

FIG. 12. The speed of sound squared of the plasma c_s^2 as a function of temperature T, for the B2 model (solid curve), compared with $(2+1)$ flavors SU(3) QCD lattice results (data points) [44].

characterized only by a sudden, but continuous, change of the thermodynamics properties.

Model B2 gives a reasonable description of $(2+1)$ QCD thermodynamics, as it can be seen in Fig. 11 (pressure p as a function of the temperature T) and in Fig. 12 (equation of state in terms of c_s^2).[8] The five-dimensional Einstein's constant $G_5 = 0.501$ is chosen to reproduce lattice data for the pressure in Fig. 11. We also note that this model provides a quantitative description of the norm of the expectation value of the Polyakov loop found on the lattice [78].

[8]We use the position of the minimum of c_s^2 to set the scale of the temperature and express T in MeV.

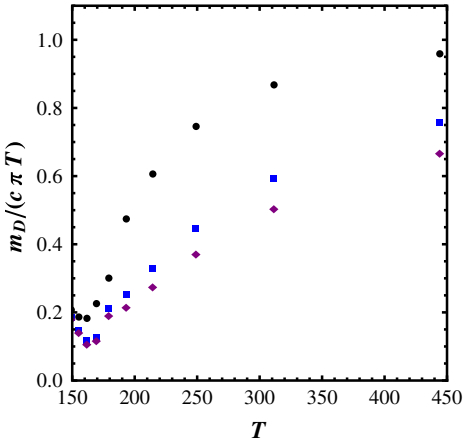

FIG. 13 (color online). Debye screening mass m_D for the model B2 with a crossover transition, normalized by the $\mathcal{N}=4$ SYM result $c\pi T$ (with $c = 3.4041$) as a function of the temperature T for $c_4 = 0.1$ (black circles), 1 (blue squares), and 10 (purple diamonds).

B. Debye screening mass

Following the same procedure employed in previous sections, we may now evaluate the Debye screening mass as a function of the temperature in this model. The results are shown in Fig. 13. The Debye screening mass m_D/T has a local minimum around $T \sim 150$ MeV showing a similar temperature dependence found for c_s^2 (Fig. 10). This minimum means, intuitively, that the plasma gets less screened (more transparent) to the strong interaction between colored heavy probes near the phase transition. Once again, larger values of c_4 show convergence and imply a faster rising to the conformal result (in this case by varying c_4 by 2 orders of magnitude, the high T values of m_D/T vary by $\sim 30\%$).

VIII. DEBYE MASS DEPENDENCE WITH η/s—GAUSS–BONNET GRAVITY

A. Action and background geometry

As a final application of the holographic evaluation of the Debye screening mass, we consider a class of bulk actions that include curvature squared corrections to the supergravity action that violate the shear viscosity bound $\eta/s \geq 1/4\pi$ [48]. The action for these gravity theories, also called Gauss–Bonnet gravity [45], is given by

$$S = \frac{1}{16\pi G_5}\int d^5x\sqrt{g}\Big[\Big(\mathcal{R}+\frac{12}{R^2}\Big)+ \\ +\frac{\lambda_{\rm GB}}{2}R^2(\mathcal{R}^2-4\mathcal{R}_{\mu\nu}\mathcal{R}^{\mu\nu}+\mathcal{R}_{\mu\nu\rho\sigma}\mathcal{R}^{\mu\nu\rho\sigma})\Big], \quad (83)$$

where $\mathcal{R}_{\mu\nu\rho\sigma}$ is the Riemann curvature tensor and $\lambda_{\rm GB}$ is a constant. In Eq. (83), the first term is the usual second-order Einstein–Hilbert action with the addition of the

cosmological constant term. The constant $\lambda_{\rm GB}$ is a measure of the size of the higher derivative corrections. The specific form the curvature squared corrections in (83) implies that the metric fluctuations in a given background still follow second-order equations.

The action (83) has an exact black brane solution [46],

$$ds^2 = \frac{R^2}{z^2}\alpha^2\left(f_{\rm GB}(z)d\tau^2 + d\vec{x}^2 + \frac{dz^2}{f_{\rm GB}(z)}\right), \tag{84}$$

where the scaling factor α is defined by

$$\alpha^2 = \frac{1}{2}\left(1+\sqrt{1-4\lambda_{\rm GB}}\right), \tag{85}$$

and the blackening factor $f_{\rm GB}$ is given by

$$f_{\rm GB}(z) = \frac{1}{2\lambda_{\rm GB}}\left[1-\sqrt{1-4\lambda_{\rm GB}\left(1-\frac{z^4}{z_h^4}\right)}\right]. \tag{86}$$

We choose our coordinate system to write the background in a Poincaré patchlike form. The z coordinate of the black brane horizon corresponds to the simple root of $f_{\rm GB}(z)$, z_h. The temperature of the black brane solution is given by $T = \alpha/(\pi R^2 z_h)$. Comparing with Eq. (84), one can see that the scaling factor means that the AdS radius is now given by αR. Finally, the 't Hooft coupling λ in this case is $\lambda = \alpha^4 R^4/\alpha'^2$. The specific forms of a and $f_{\rm GB}$ imply that $\lambda_{\rm GB} < 1/4$. Another constraint is given by imposing causality at the boundary, which implies $\lambda_{\rm GB} \leq 9/100$ [50].

The shear viscosity/entropy density ratio η/s in this model is related to $\lambda_{\rm GB}$ by [51]

$$\frac{\eta}{s} = \frac{1}{4\pi}(1-4\lambda_{\rm GB}). \tag{87}$$

If $\lambda_{\rm GB} > 0$ one has $\eta/s < 1/4\pi$—the conjectured viscosity bound for gauge theories with gravity duals is then violated. Imposing $\lambda_{\rm GB} \leq 9/100$ implies $\frac{4\pi\eta}{s} \geq 16/25$.

B. Debye screening mass

We have not specified the string theory construction that leads to Gauss–Bonnet gravity, but such a discussion can be found in Ref. [88]. The only field that can contribute to the channel used to define the Debye mass is the axion, which is once again trivial in this background. The action for the axion fluctuations (10) including only two derivatives is (this is still a conformal system, and, thus, $\mathcal{Z} = 1$)

$$S = \frac{\alpha}{32\pi G_5}\int d^5x e^{5\mathcal{A}}(\partial a)^2, \tag{88}$$

where $\mathcal{A}(z) = \log(R/z)$. Apart from the constant factor of proportionality α in the action, this is the same action that would be obtained with a background of the form (11). So our equation of motion is still Eq. (15), with $\mathcal{B} = 3/2\log(z/R)$. As in Sec. III, we use the dimensionless variable $y = z/z_h$, which yields the dimensionless mass $\tilde{M} = M/(\pi T)$.

Also, one can check that in this case the potential $\mathcal{V}(y)$ in Eq. (15) has the same asymptotic form near the boundary, namely $\mathcal{V}(y\to 0) = 15/(4y^2)$—the leading term in $1/y$ is not changed. So, the asymptotic solutions are the same, and all the tools used in Sec. III can be applied in this case without modifications. To obtain the Debye screening mass as a function of η/s, we analyze several values of $\lambda_{\rm GB}$ and then use Eq. (87) to obtain the corresponding values of η/s.

We also compare our numerical results with the phenomenological procedure pursued in Ref. [52]. In that paper, we evaluated in the strongly coupled plasma dual to Gauss–Bonnet gravity the expectation value of the rectangular Wilson-loop operator at finite temperature, which yields the potential energy $V_{Q\bar{Q}}$ of a heavy quark-antiquark pair that depends on η/s [89]. Using fits for the real part of the potential of the form

$$\frac{{\rm Re}V_{Q\bar{Q}}}{\sqrt{\tilde{\lambda}}T} = -\tilde{C}_1\frac{e^{-\frac{\tilde{m}_D}{T}(LT)}}{(LT)^{\delta}} + \tilde{C}_2, \tag{89}$$

where L is the interquark distance while $\tilde{C}_1$, δ, and $\tilde{m}_D$ were taken as fit parameters (we note that $\tilde{C}_2 = -1/\alpha^2$ by our regularization procedure), we found an estimate for the Debye screening mass $\tilde{m}_D$. For $\lambda_{\rm GB} = 0$ we found $\tilde{m}_D = 3.79\pi T$, in reasonable agreement with the result of Eq. (19).

We present the results for the Debye mass m_D (normalized by the SYM value) as a function of the η/s in Fig. 14.

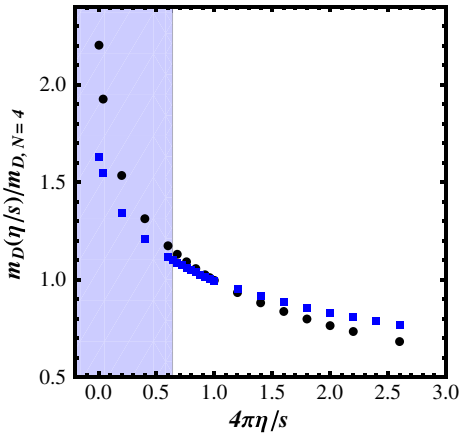

FIG. 14 (color online). Debye mass m_D for the Gauss–Bonnet gravity dual, as a function of η/s, normalized by the $\mathcal{N} = 4$ SYM value. The black circles correspond to the results obtained by computing the lightest CT-odd mode; the blue squares are the results obtained by fits to the heavy quark-antiquark potential evaluated holographically [52]. The shaded region corresponds to values of η/s which violate the causality bound [50,51].

We note that we have not restricted our calculations to the interval $\frac{4\pi\eta}{s} \geq 16/25$ as required by causality but considered, for completeness, $\eta/s \geq 0$. One can see that for increasing η/s the interaction between colored external probes in the plasma is less screened. This is reasonable, at least from the point of view of a weakly coupled plasma since η/s is roughly proportional to the mean free path of momentum isotropization of the plasma and changing η/s does not change the number of degrees of freedom of the system. Thus, less screening should correspond to a larger mean free path and, thus, to a larger η/s. We also note the unexpected coincidence between the results obtained by finding the lightest CT-odd mode and those obtained following the simple phenomenological procedure using the heavy quark potential described in the previous paragraph.

IX. DISCUSSION AND CONCLUSIONS

In this paper we have identified the Debye screening mass m_D in non-Abelian gauge theories at strong coupling with the lightest CT-odd mode in the spectrum (associated with the operator $\mathrm{Tr}F_{\mu\nu}\tilde{F}^{\mu\nu}$), following Refs. [9,23]. We used this prescription to holographically evaluate the Debye screening mass for a class of gravity duals involving the metric and a scalar field. Besides the conformal cases of $\mathcal{N}=4$ SYM at strong coupling and the gauge theory dual to Gauss–Bonnet gravity (where the scalar field in the bulk vanishes), we investigated in detail an analytic bottom-up model with a first-order confinement/deconfinement transition (model A) and two bottom-up holographic models that describe the thermodynamics of QCD as seen on the lattice—models B1 (pure glue, first-order phase transition) and B2 (QCD, crossover transition).

The calculation of m_D/T in both models for a pure Yang–Mills plasma with a first-order phase transition at T_c, models A and B1, revealed some interesting features. Both models approach the conformal limit for $T \gg T_c$ and exhibit relatively little sensitivity to the axion coupling prefactor $\mathcal{Z}$. The most remarkable feature of both models is the discontinuity of m_D/T at the critical temperature T_c—m_D jumps from 0 in the thermal gas phase ($T < T_c$) to a nonzero value at $T = T_c$. This behavior for m_D/T in a pure $\mathrm{SU}(N_c)$ Yang–Mills plasma is consistent with previous lattice studies [16].

We also computed the expectation value of the Polyakov loop in these models, finding an impressive agreement with lattice results [53] even for $N_c = 3$. Moreover, even model A, which does not provide an adequate quantitative description of $\mathrm{SU}(3)$ thermodynamics, yields a reasonable description for the Polyakov loop. This suggests that the Polyakov loop is largely insensitive to a variation in the number of colors N_c in a pure glue plasma and that even $N_c = 3$ may be reasonably described by a large-N_c expansion [53]. Moreover, it would be interesting to identify more clearly what is the specific nonperturbative mechanism present in these holographic models that is responsible for this simultaneous description of lattice QCD thermodynamics and the expectation value of the polyakov loop.

Model B2 provides a reasonable description of the thermodynamics of $(2+1)$ QCD.[9] The Debye screening mass, correspondingly, satisfies $m_D(T) > 0$ strictly and is always continuous. Near the crossover phase transition region at $T \sim 150$ MeV, we see a minimum of m_D/T (Fig. 13). This minimum resembles, qualitatively, that found for the speed of sound squared $c_s^2(T)$, as shown in Fig. 12. For all the models, A, B1, and B2, the conformal regime is reached from below; that is, $m_D(T) < c\pi T$. The minimum of m_D/T near the phase transition may have consequences for the energy loss of colored probes in the plasma [94]. Also, such a minimum implies that correlations in the medium are less screened, which effectively increases the range of interactions, and this may be responsible for the (expected) small value of η/s around $T \sim 150$ MeV [95–98]. Equivalently, in this temperature range, the expectation value of the Polyakov loop becomes small, and, within the framework of the semi-QGP model [56,99], such a reduction may also lead to a suppression of η/s [100,101].

The Debye screening mass of $\mathcal{N}=4$ SYM at strong coupling, $m_D = 3.4041\pi T$, extracted using the procedure of Ref. [9], yields a result that is remarkably close to the crude estimate used in Ref. [52] where fits to the heavy quark-antiquark potential gave $m_D = 3.79\pi T$. However, this coincidence should be interpreted with caution since, as discussed in Ref. [52], the heavy quark-antiquark potential in $\mathcal{N}=4$ SYM at strong coupling is not exponentially screened (for small values of LT) as required to obtain the Debye screening mass from $V_{Q\bar{Q}}$.

By considering a gravity theory with higher-order derivatives such that the gauge plasma does not satisfy $\eta/s = 1/(4\pi)$, namely Gauss–Bonnet gravity, we have evaluated the dependence of m_D/T with η/s, as shown in Fig. 14. We found that in this case less screening is seen as η/s is increased. It would be interesting to check this result in other strongly coupled gauge theories. In particular, one could consider gravity duals that correspond to gauge theories in which $\eta/s < 1/(4\pi)$ still in the context of applications to the QGP. For example, one can consider axion induced anisotropic deformations of $\mathcal{N}=4$ SYM [102,103] or strongly coupled $\mathcal{N}=4$ SYM subjected to an external magnetic field [104,105]. However, the prescription of Ref. [9] cannot be straightforwardly applied to

[9]We should, however, emphasize that the gauge theory described by this gravity dual does not strictly possesses fermions in the fundamental representation. Those can be included using D-branes in the bulk geometry [90,91]. See Ref. [92] for a general review and Ref. [93] for a study of the Veneziano limit in bottom-up constructions.

these theories because they are not invariant by CP—P invariance is explicitly broken by the inclusion of the axion field in Ref. [102] and by the presence of an external magnetic field in Ref. [105].

ACKNOWLEDGMENTS

We thank M. Panero for making available to us the lattice results for the Polyakov loop from Ref. [53] and for discussions about the renormalization scheme dependence of Polyakov loops. We also thank A. Dumitru for very insightful comments on the manuscript and A. Ficnar for discussions regarding the numerical solutions of Einstein's equations. The authors thank Fundação de Amparo à Pesquisa do Estado de São Paulo (FAPESP) and Conselho Nacional de Desenvolvimento Científico e Tecnológico (CNPq) for support.

APPENDIX A: GAUGE CHOICES FOR MODELS B1 AND B2

As mentioned in the main text, for the models B1 and B2, the Gubser gauge (44), while adequate for studying the thermodynamics, is not convenient for evaluating Polyakov and Wilson loops or finding the glueball spectrum (as done in Appendix B). For these purposes, it is convenient to change to the conformal gauge given by

$$ds^2 = e^{2\tilde{A}(z)}\left(\tilde{h}(z)d\tau^2 + d\vec{x}^2 + \frac{dz^2}{\tilde{h}(z)}\right). \tag{A1}$$

Comparing Eq. (A1) with Eq. (44), we see that the following relation must hold among the metric functions:

$$\frac{dz}{d\phi} = e^{B-A}. \tag{A2}$$

We require that the asymptotic AdS_5 is located at $z = 0$ and that the horizon is at $z = z_h$. The solution of Eq. (A2) that satisfies these requirements is

$$z(\phi) = \int_0^{\phi} d\tilde{\phi} e^{B(\tilde{\phi})-A(\tilde{\phi})}. \tag{A3}$$

We can invert (numerically) Eq. (A3) to get $\phi(z)$. Then, the functions $\tilde{A}(z)$ and $\tilde{h}(z)$ are given by $\tilde{A}(z) = A(\phi(z))$ and $\tilde{h}(z) = h(\phi(z))$.

APPENDIX B: GLUEBALL SPECTRA IN MODEL B1

In this section we compute the glueball spectra for model B1, which displays confinement at $T = 0$. The parameters used in the scalar potential in this model are given in Table II.

Let us briefly review the numerical procedure for finding the vacuum geometry and the glueball spectra. One first numerically integrates the equations of motion (58) subject to the boundary condition (59); then, we search, numerically, for the eigenvalues of the Schrödinger's equation (16), as described in the main text. To find the spectra, we change the metric from the $z = \phi$ gauge (44) to the conformal gauge, as described in Appendix A. The potential for Schrödinger's equation is given by Eq. (17), where $\mathcal{B}$ depends on whether we are dealing with the scalar $J^{PC} = 0^{++}$ glueballs, tensor $J^{PC} = 2^{++}$ glueballs, or pseudoscalar $J^{PC} = 0^{-+}$ glueballs [33,106],

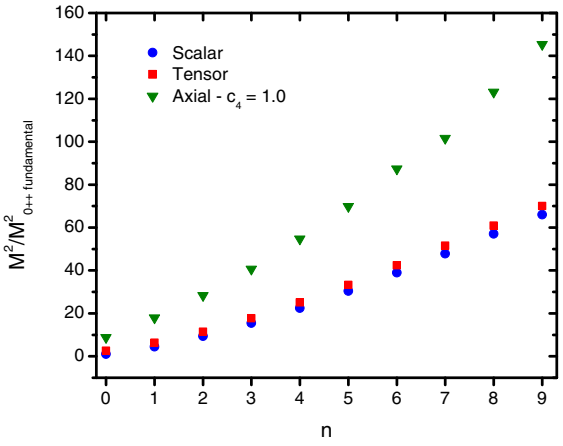

FIG. 15 (color online). Glueball spectra in the model B1. The glueball masses are normalized by the mass of the fundamental $J^{PC} = 0^{++}$ glueball. n indicates the order of the excited state; $n = 0$ is the fundamental state.

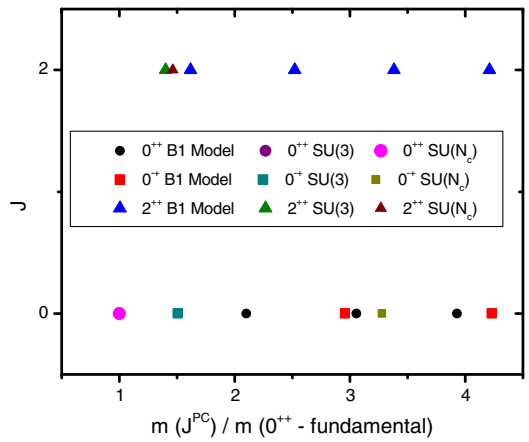

FIG. 16 (color online). Chew–Frautschi plot of the glueball spectra, comparing results from model B1 with lattice results for SU(3) [107,108] and large-N_c SU(N_c) [109,110] Yang–Mills theory.

$$\begin{aligned}
&(\text{scalar})0^{++} \quad \mathcal{B}(z) = \frac{3}{2}\mathcal{A}(z) + \frac{1}{2}\log X(z),\\
&(\text{tensor})2^{++} \quad \mathcal{B}(z) = \frac{3}{2}\mathcal{A}(z),\\
&(\text{axial}) \quad 0^{-+}\mathcal{B}(z) = \frac{3}{2}\mathcal{A}(z) + \frac{1}{2}\log \mathcal{Z}(\lambda(z)).
\end{aligned} \tag{B1}$$

In Eq. (B1), $X(z)$ is defined by

$$X(z) \equiv \frac{d\Phi/dz}{3\mathcal{A}(z)}, \tag{B2}$$

where $\Phi = \sqrt{3/8}\phi(z)$ while $\lambda(z) = e^{\phi(z)}$, with $Z(\lambda)$ still given by Eq. (40). For a comparison with lattice results, we normalize the spectrum by the fundamental 0^{++} glueball mass.

Our results are shown in Figs. 15 and 16. For comparison we used lattice results for the glueball spectra in pure Yang–Mills with gauge groups SU(3) [107,108] and SU(N_c) in the large-N_c limit [109,110]. We see in Fig. 15 that linear Regge trajectories are achieved for $n > 4$. Also, we note that the axial glueball has little sensitivity to the choice of c_4—in the interval $c_4 = 0.1$ to $c_4 = 10$, the masses are almost degenerate. For this reason, in Fig. 15 we show only the results for $c_4 = 1$. Comparing with lattice results (Fig. 16), we see that reasonable agreement is found for the tensor glueball among all calculations. The axial glueball of model B1 and large-N_c SU(N_c) Yang–Mills are both reasonably close; however, both axial glueball masses are off by a factor of 2 when compared with the SU(3) Yang–Mills fundamental axial glueball. This contrasts with the results found for the holographic Polyakov loop in Sec. VI B, where the results were relatively insensitive to N_c.

[1] T. Matsui and H. Satz, Phys. Lett. B **178**, 416 (1986).
[2] E. V. Shuryak, Phys. Rep. **61**, 71 (1980).
[3] D. J. Gross, R. D. Pisarski, and L. G. Yaffe, Rev. Mod. Phys. **53**, 43 (1981).
[4] J. I. Kapusta and C. Gale, *Finite-Temperature Field Theory: Principles and Applications* (Cambridge University Press, Cambridge, England, 2006), p. 428.
[5] S. Nadkarni, Phys. Rev. D **33**, 3738 (1986).
[6] A. K. Rebhan, Phys. Rev. D **48**, R3967 (1993).
[7] E. Braaten and A. Nieto, Phys. Rev. Lett. **73**, 2402 (1994).
[8] A. K. Rebhan, Nucl. Phys. **B430**, 319 (1994).
[9] P. B. Arnold and L. G. Yaffe, Phys. Rev. D **52**, 7208 (1995).
[10] K. Kajantie, M. Laine, J. Peisa, A. Rajantie, K. Rummukainen, and M. E. Shaposhnikov, Phys. Rev. Lett. **79**, 3130 (1997).
[11] S. Datta and S. Gupta, Phys. Lett. B **471**, 382 (2000).
[12] S. Datta and S. Gupta, Nucl. Phys. **B534**, 392 (1998).
[13] S. Datta and S. Gupta, Phys. Rev. D **67**, 054503 (2003).
[14] M. Laine and O. Philipsen, Phys. Lett. B **459**, 259 (1999).
[15] A. Hart, M. Laine, and O. Philipsen, Nucl. Phys. **B586**, 443 (2000).
[16] A. Nakamura, T. Saito, and S. Sakai, Phys. Rev. D **69**, 014506 (2004).
[17] A. Cucchieri, F. Karsch, and P. Petreczky, Phys. Lett. B **497**, 80 (2001).
[18] A. Cucchieri, D. Dudal, T. Mendes, and N. Vandersickel, arXiv:1202.0639.
[19] R. Aouane, F. Burger, E.-M. Ilgenfritz, M. Müller-Preussker, and A. Sternbeck, Phys. Rev. D **87**, 114502 (2013).
[20] P. J. Silva, O. Oliveira, P. Bicudo, and N. Cardoso, Phys. Rev. D **89**, 074503 (2014).
[21] M. Laine and M. Vepsalainen, J. High Energy Phys. 09 (2009) 023.
[22] P. Chakraborty, M. G. Mustafa, and M. H. Thoma, Phys. Rev. D **85**, 056002 (2012).
[23] D. Bak, A. Karch, and L. G. Yaffe, J. High Energy Phys. 08 (2007) 049.
[24] C. Hoyos, S. Paik, and L. G. Yaffe, J. High Energy Phys. 10 (2011) 062.
[25] A. Singh and A. Sinha, Nucl. Phys. **B864**, 167 (2012).
[26] J. M. Maldacena, Adv. Theor. Math. Phys. **2**, 231 (1998); [Int. J. Theor. Phys. **38**, 1113 (1999)].
[27] E. Witten, Adv. Theor. Math. Phys. **2**, 253 (1998).
[28] E. Witten, Adv. Theor. Math. Phys. **2**, 505 (1998).
[29] S. S. Gubser, I. R. Klebanov, and A. M. Polyakov, Phys. Lett. B **428**, 105 (1998).
[30] C. Csaki, H. Ooguri, Y. Oz, and J. Terning, J. High Energy Phys. 01 (1999) 017.
[31] R. de Mello Koch, A. Jevicki, M. Mihailescu, and J. P. Nunes, Phys. Rev. D **58**, 105009 (1998).
[32] U. Gursoy and E. Kiritsis, J. High Energy Phys. 02 (2008) 032.
[33] U. Gursoy, E. Kiritsis, and F. Nitti, J. High Energy Phys. 02 (2008) 019.
[34] U. Gursoy, E. Kiritsis, L. Mazzanti, and F. Nitti, Phys. Rev. Lett. **101**, 181601 (2008).
[35] U. Gursoy, E. Kiritsis, L. Mazzanti, and F. Nitti, J. High Energy Phys. 05 (2009) 033.
[36] U. Gursoy, E. Kiritsis, L. Mazzanti, and F. Nitti, Nucl. Phys. **B820**, 148 (2009).
[37] K. Kajantie, M. Krssak, M. Vepsalainen, and A. Vuorinen, Phys. Rev. D **84**, 086004 (2011).
[38] S. S. Gubser and A. Nellore, Phys. Rev. D **78**, 086007 (2008).
[39] S. S. Gubser, A. Nellore, S. S. Pufu, and F. D. Rocha, Phys. Rev. Lett. **101**, 131601 (2008).
[40] S. S. Gubser, S. S. Pufu, and F. D. Rocha, J. High Energy Phys. 08 (2008) 085.

[41] G. Boyd, J. Engels, F. Karsch, E. Laermann, C. Legeland, M. Lutgemeier, and B. Petersson, Nucl. Phys. **B469**, 419 (1996),
[42] M. Panero, Phys. Rev. Lett. **103**, 232001 (2009).
[43] S. Borsanyi, G. Endrodi, Z. Fodor, S. D. Katz, and K. K. Szabo, J. High Energy Phys. 07 (2012) 056.
[44] S. Borsanyi, G. Endrodi, Z. Fodor, A. Jakovac, S. D. Katz, S. Krieg, C. Ratti, and K. K. Szabo, J. High Energy Phys. 11 (2010) 077.
[45] B. Zwiebach, Phys. Lett. **156B**, 315 (1985).
[46] R.-G. Cai, Phys. Rev. D **65**, 084014 (2002).
[47] G. Policastro, D. T. Son, and A. O. Starinets, Phys. Rev. Lett. **87**, 081601 (2001).
[48] P. Kovtun, D. T. Son, and A. O. Starinets, Phys. Rev. Lett. **94**, 111601 (2005).
[49] A. Buchel and J. T. Liu, Phys. Rev. Lett. **93**, 090602 (2004).
[50] M. Brigante, H. Liu, R. C. Myers, S. Shenker, and S. Yaida, Phys. Rev. Lett. **100**, 191601 (2008).
[51] M. Brigante, H. Liu, R. C. Myers, S. Shenker, and S. Yaida, Phys. Rev. D **77**, 126006 (2008).
[52] S. I. Finazzo and J. Noronha, J. High Energy Phys. 11 (2013) 042.
[53] A. Mykkanen, M. Panero, and K. Rummukainen, J. High Energy Phys. 05 (2012) 069.
[54] U. Gürsoy, I. Iatrakis, E. Kiritsis, F. Nitti, and A. O'Bannon, J. High Energy Phys. 02 (2013) 119.
[55] P. K. Kovtun and A. O. Starinets, Phys. Rev. D **72**, 086009 (2005).
[56] R. D. Pisarski, Phys. Rev. D **62**, 111501 (2000).
[57] A. Dumitru, Y. Hatta, J. Lenaghan, K. Orginos, and R. D. Pisarski, Phys. Rev. D **70**, 034511 (2004).
[58] R. D. Pisarski, Phys. Rev. D **74**, 121703 (2006).
[59] A. Dumitru, Y. Guo, Y. Hidaka, C. P. K. Altes, and R. D. Pisarski, Phys. Rev. D **86**, 105017 (2012).
[60] M. Bianchi, D. Z. Freedman, and K. Skenderis, Nucl. Phys. **B631**, 159 (2002).
[61] K. Skenderis, Classical Quantum Gravity **19**, 5849 (2002).
[62] A. M. Polyakov, Phys. Lett. **72B**, 477 (1978).
[63] G. 't Hooft, Nucl. Phys. **B138**, 1 (1978); **B153**, 141 (1979).
[64] B. Svetitsky and L. G. Yaffe, Nucl. Phys. **B210**, 423 (1982).
[65] L. D. McLerran and B. Svetitsky, Phys. Lett. **98B**, 195 (1981); Phys. Rev. D **24**, 450 (1981).
[66] J. M. Maldacena, Phys. Rev. Lett. **80**, 4859 (1998).
[67] A. Brandhuber, N. Itzhaki, J. Sonnenschein, and S. Yankielowicz, Phys. Lett. B **434**, 36 (1998).
[68] S.-J. Rey, S. Theisen, and J.-T. Yee, Nucl. Phys. **B527**, 171 (1998).
[69] J. Noronha, Phys. Rev. D **81**, 045011 (2010).
[70] J. Noronha, Phys. Rev. D **82**, 065016 (2010).
[71] J. Noronha and A. Dumitru, Phys. Rev. Lett. **103**, 152304 (2009).
[72] S. Gradshteyn and I. M. Ryzhik, *Table of Integrals, Series, and Products*, 7th ed., edited by A. Jeffrey and D. Zwillinger (Academic, New York, 2007).
[73] K. Pilch and N. P. Warner, Nucl. Phys. **B594**, 209 (2001).
[74] A. Buchel and J. T. Liu, J. High Energy Phys. 11 (2003) 031.
[75] A. Buchel, S. Deakin, P. Kerner, and J. T. Liu, Nucl. Phys. **B784**, 72 (2007).
[76] S. I. Finazzo and J. Noronha, Phys. Rev. D **89**, 106008 (2014).
[77] A. Amato, G. Aarts, C. Allton, P. Giudice, S. Hands, and J. I. Skullerud, Phys. Rev. Lett. **111**, 172001 (2013).
[78] A. Ficnar, J. Noronha, and M. Gyulassy, Nucl. Phys. **A855**, 372 (2011).
[79] A. Ficnar, J. Noronha, and M. Gyulassy, J. Phys. G **38**, 124176 (2011).
[80] A. Ficnar, J. Noronha, and M. Gyulassy, Nucl. Phys. **A910–911**, 252 (2013).
[81] D. Li and M. Huang, J. High Energy Phys. 11 (2013) 088.
[82] D. Li, S. He, and M. Huang, arXiv:1411.5332.
[83] A. Karch, E. Katz, D. T. Son, and M. A. Stephanov, Phys. Rev. D **74**, 015005 (2006).
[84] H. A. Chamblin and H. S. Reall, Nucl. Phys. **B562**, 133 (1999).
[85] Y. Aoki, G. Endrodi, Z. Fodor, S. D. Katz, and K. K. Szabo, Nature **443**, 675 (2006).
[86] S. S. Gubser, Adv. Theor. Math. Phys. **4**, 679 (2000).
[87] F. Zuo, J. High Energy Phys. 06 (2014) 143.
[88] A. Buchel, R. C. Myers, and A. Sinha, J. High Energy Phys. 03 (2009) 084.
[89] J. Noronha and A. Dumitru, Phys. Rev. D **80**, 014007 (2009).
[90] A. Karch and E. Katz, J. High Energy Phys. 06 (2002) 043.
[91] M. Kruczenski, D. Mateos, R. C. Myers, and D. J. Winters, J. High Energy Phys. 07 (2003) 049.
[92] J. Erdmenger, N. Evans, I. Kirsch, and E. Threlfall, Eur. Phys. J. A **35**, 81 (2008).
[93] T. Alho, M. Järvinen, K. Kajantie, E. Kiritsis, C. Rosen, and K. Tuominen, J. High Energy Phys. 04 (2014) 124.
[94] A. Dumitru and R. D. Pisarski, Phys. Lett. B **525**, 95 (2002).
[95] T. Hirano and M. Gyulassy, Nucl. Phys. **A769**, 71 (2006).
[96] L. P. Csernai, J. I. Kapusta, and L. D. McLerran, Phys. Rev. Lett. **97**, 152303 (2006).
[97] J. Noronha-Hostler, J. Noronha, and C. Greiner, Phys. Rev. Lett. **103**, 172302 (2009).
[98] J. Noronha-Hostler, J. Noronha, and C. Greiner, Phys. Rev. C **86**, 024913 (2012).
[99] Y. Hidaka and R. D. Pisarski, Phys. Rev. D **80**, 036004 (2009).
[100] Y. Hidaka and R. D. Pisarski, Phys. Rev. D **78**, 071501 (2008).
[101] Y. Hidaka and R. D. Pisarski, Phys. Rev. D **81**, 076002 (2010).
[102] D. Mateos and D. Trancanelli, Phys. Rev. Lett. **107**, 101601 (2011).
[103] A. Rebhan and D. Steineder, Phys. Rev. Lett. **108**, 021601 (2012).
[104] E. D'Hoker and P. Kraus, J. High Energy Phys. 10 (2009) 088.
[105] R. Critelli, S. I. Finazzo, M. Zaniboni, and J. Noronha, Phys. Rev. D **90**, 066006 (2014).
[106] E. Kiritsis and F. Nitti, Nucl. Phys. **B772**, 67 (2007).
[107] C. J. Morningstar and M. J. Peardon, Phys. Rev. D **60**, 034509 (1999).
[108] Y. Chen *et al.*, Phys. Rev. D **73**, 014516 (2006),
[109] B. Lucini and M. Teper, J. High Energy Phys. 0106 (2001) 050.
[110] B. Lucini, A. Rago, and E. Rinaldi, J. High Energy Phys. 08 (2010) 119.